Mass Spectrometric Analysis of Nitroxyl-Mediated Protein Modification: Comparison of Products Formed with Free and Protein-Based Cysteines†

Biao Shen and Ann M. English*

Department of Chemistry and Biochemistry, Concordia University, 7141 Sherbrooke Street West, Montreal, Quebec, Canada H4B 1R6

Received April 22, 2005; Revised Manuscript Received August 15, 2005

ABSTRACT: Although biologically active, nitroxyl (HNO) remains one of the most poorly studied NO_x. Protein-based thiols are suspected targets of HNO, forming either a disulfide or sulfinamide ($RSONH_2$) through an *N*-hydroxysulfenamide (RSNHOH) addition product. Electrospray ionization mass spectrometry (ESI-MS) is used here to examine the products formed during incubation of thiol proteins with the HNO donor, Angeli's salt (AS; $Na_2N_2O_3$). Only the disulfide, cystine, was formed in incubates of 15 mM free Cys with equimolar AS at pH 7.0−7.4. In contrast, the thiol proteins (120−180 μM), human calbindin D_{28k} (HCalB), glyceraldehyde-3-phosphate dehydrogenase (GAPDH), and bovine serum albumin (BSA) gave four distinct types of derivatives in incubates containing 0.9−2.5 mM AS. Ions at M + n × 31 units were detected in the ESI mass spectra of intact HCalB (n = 1−5) and GAPDH (n = 2), indicating conversion of thiol groups on these proteins to $RSONH_2$ (+31 units). An ion at M + 14 dominated the mass spectrum of BSA, and intramolecular sulfinamide cross-linking of Cys34 to one of its neighboring Lys or Arg residues would account for this mass increase. Low abundant M + 14 adducts were observed for HCalB, which additionally formed mixed disulfides when free Cys was present in the AS incubates. Cys149 and Cys153 formed an intramolecular disulfide in the AS/GAPDH incubates. Since AS also produces nitrite above pH 5 ($HN_2O_3^- \rightarrow HNO + NO_2^-$), incubation with $NaNO_2$ served to confirm that protein modification was HNO-mediated, and prior blocking with the thiol-specific reagent, *N*-ethylmaleimide, demonstrated that thiols are the targets of HNO. The results provide the first systematic characterization of HNO-mediated derivatization of protein thiols.

Since the discoveries of nitric oxide (NO) biosynthesis in mammalian cells and the diverse biological activity associated with NO and NO-derived species, there has been extensive interest in the chemistry and biology of nitrogen oxides (NO_x). It is now established that the generation of endogenous NO_x represents important biochemical signaling pathways, critical components of the immune response, and potential pathophysiological events. To date, NO has been shown to regulate processes such as platelet function, leukocyte recruitment, mitochondrial respiration, vascular tone, and cardiac function (*1*, *2*).

The one-electron reduction product of NO, nitroxyl (NO^-), or more likely its conjugate acid, HNO,[1] with a pK_a >11 (*3*, *4*), is known to be formed under physiological conditions. In fact, there are reports that HNO is produced by nitric oxide synthase (NOS) under certain circumstances (*5*) and via the metabolism of the decoupled NOS product *N*-hydroxy-L-arginine under oxidative stress (*6*). HNO also is formed under nitrosative stress (*7*) and by thiolysis of *S*-nitrosothiols (RSNO) following nucleophilic attack on the SNO sulfur (*8*, *9*). The direct reduction of NO by mitochondrial cytochrome *c* (*10*), xanthine oxidase (*11*), Cu- and Mn-containing superoxide dismutases (*12*), and ubiquinol (*13*) is among further reactions reported to generate HNO.

Several reports indicate that HNO is electrophilic around neutral pH (*4*, *8*), and recent theoretical studies predict highly favorable reactions with thiols (RSH) and amines (*4*). Electrophilic attack on RSH produces an *N*-hydroxysulfenamide addition product (RSNHOH) that can react with a second RSH to yield the corresponding disulfide RSSR and hydroxylamine (NH_2OH) (*8*, *14*) or spontaneously eliminate hydroxide ion to form a stable sulfinamide following hydration and deprotonation (*8*) (Scheme 1).

Scheme 1

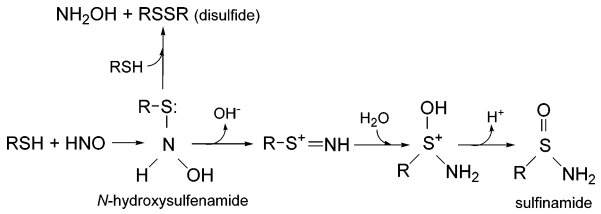

† This study was supported by grants from the Canadian Institutes of Health Research (CIHR) and the Natural Sciences and Engineering Research Council (NSERC) of Canada to A.M.E.

* To whom correspondence should be addressed. E-mail: english@vax2.concordia.ca. Tel: (514) 848-2424 ext 3338. Fax: (514) 848-2868.

[1] Abbreviations: AS, Angeli's salt (sodium trioxodinitrate); BSA, bovine serum albumin; Cys, L-cysteine; (Cys-H)•, cysteinyl radical; DTNB, 5,5′-dithiobis(2-nitrobenzoic acid); DTT, dithiothreitol; ESI-MS, electrospray ionization mass spectrometry; GAPDH, glyceraldehyde-3-phosphate dehydrogenase; GSNO, *S*-nitrosoglutathione; HCalB, human brain calbindin D_{28k}; HNO, nitroxyl; NEM, *N*-ethylmaleimide; Q-ToF, quadrupole time of flight; RSH, thiol; RSNO, *S*-nitrosothiol.

10.1021/bi0507478 CCC: $30.25
Published on Web 09/29/2005

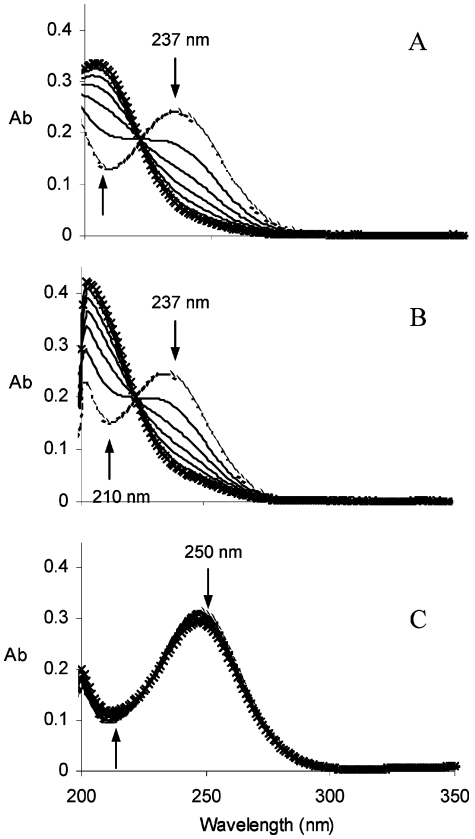

FIGURE 1: AS decomposition at 22 °C vs pH. Absorption spectra of 30 μM AS in (A) water at pH 5.5, (B) 50 mM Tris-HCl buffer at pH 7.4, and (C) 10 mM NaOH. Experimental conditions: For (A) and (B), a 0.5 μL aliquot of AS stock in 10 mM NaOH was diluted 10^3-fold into water and buffer, respectively. The spectra recorded in 1 cm cuvettes at $t = 0$ (dotted line), 5, 10, 15, 20, 25, and 30 min ($\times$ symbols) are shown. The arrows indicate the decay of AS absorption at 237 nm (pH 5.5 and 7.4) and 250 nm (10 mM NaOH) and the growth of absorption at 210 nm due to the nitrite ion, NO_2^- (*69*).

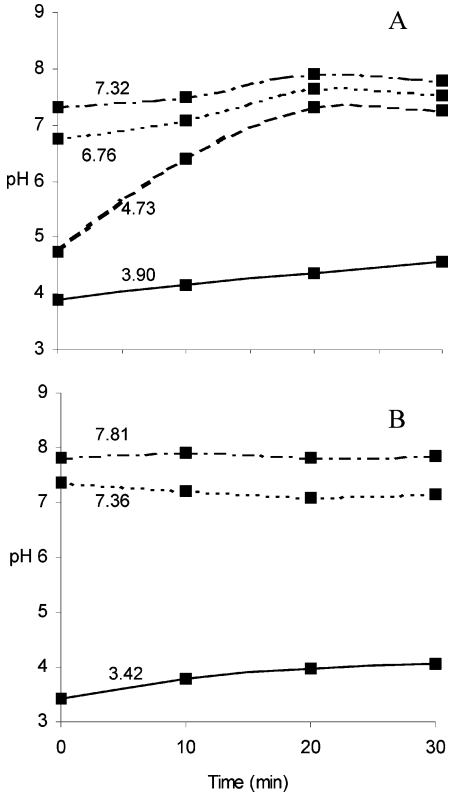

FIGURE 2: Changes in pH of the AS/Cys and $NaNO_2$/Cys incubates vs time. Cys (15 mM) was incubated with (A) 15 mM AS and (B) 15 mM $NaNO_2$ in water at room temperature. Experimental procedures: The initial pHs were adjusted to the values indicated on the plots with 1 N HCl or 1 N NaOH. The squares indicate the pH values measured at 10 min intervals using a micro pH electrode, and the connecting lines were added to clarify the variation in pH in each incubate.

Consistent with Scheme 1, HNO has been found to be a potent inhibitor of thiol-containing enzymes including aldehyde dehydrogenase (ALDH) and GAPDH (*15*, *16*). It attenuates the activity of the NMDA receptor to provide neuroprotection and inhibits activation of the yeast transcription factor, Ace1, via thiol modification (*17*, *18*). These studies indicate that protein sulfhydryl groups may be major targets of HNO donors as has been demonstrated for NO donors (*19*). Nonetheless, NO and HNO donors elicit distinct responses under a variety of biological conditions in vitro and in vivo. For example, exposure to NO donors at the onset of cardiac reperfusion is protective whereas HNO donors increase tissue damage (*5*, *20*). Under different circumstances HNO donors can promote smooth muscle relaxation (*21*) and provide thiol-sensitive myocardial protective effects that resemble early preconditioning (*22*).

The widely used (*15*, *16*, *22*−*26*) Angeli's salt (AS, sodium trioxodinitrate, $Na_2N_2O_3$) is currently the preferred HNO donor for studies on biomolecules and biological systems. Its monoprotonated form spontaneously releases HNO under physiological conditions (*27*):

$$HN_2O_3^- \rightarrow HNO + NO_2^- \quad (1)$$

Piloty's acid (benzenesulfohydroxamic acid) also spontaneously releases HNO but only in anaerobic and basic media. This acid is subject to rapid oxidation in air, yielding NO rather than HNO (*28*−*30*).

Despite the growing awareness of the biological importance of HNO (*31*), the modifications of biomolecules by HNO donors have not been chemically characterized to date. In the present study, we report the electrospray ionization (ESI) mass spectra of AS incubates with free Cys and with sulfhydryl-containing proteins that form well-characterized products with NO donors. The spectra reveal that the disulfide, cystine, is formed exclusively on incubation of free Cys with AS at neutral pH. In contrast, bovine serum albumin (BSA), glyceraldehyde-3-phosphate dehydrogenase (GAPDH), and recombinant human brain calbindin D_{28k} (HCalB), which contain one, four, and five free Cys residues, respectively, are modified in the AS incubates to give a number of distinct mass adducts. Control incubates with $NaNO_2$ are used to differentiate the products formed on RSH reaction with HNO and NO_2^- since AS releases both of these NO_x (eq 1). While the local environment of a sulfhydryl group dictates the specific HNO-mediated protein modification found, overall the results are consistent with HNO acting as an avid thiophilic electrophile.

MATERIALS AND METHODS

Materials and Solutions. Stock 15−250 mM solutions of Angeli's salt (AS; Cayman) were prepared in 10 mM NaOH,

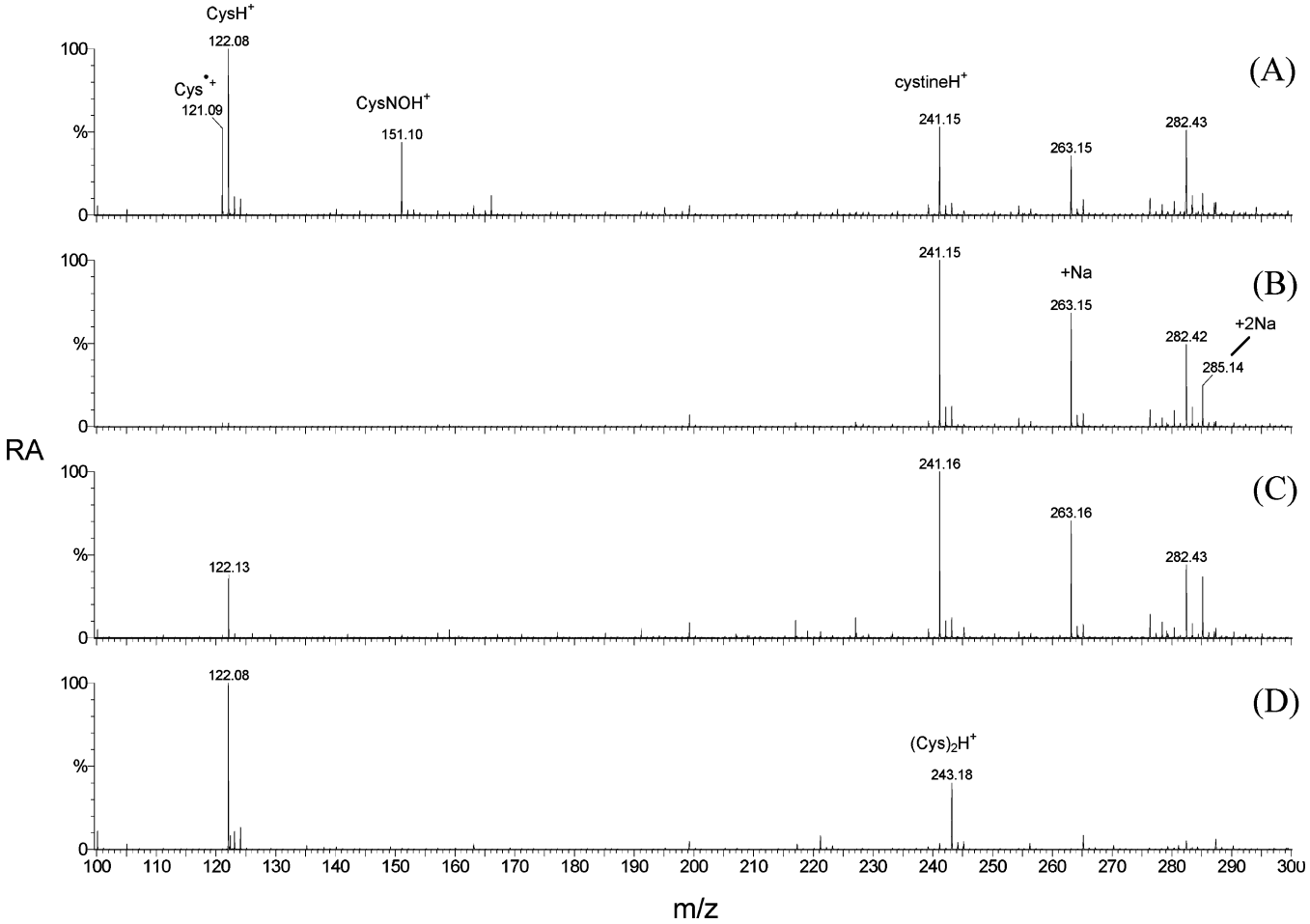

FIGURE 3: Effects of pH on the ESI mass spectra of 30 min AS/Cys incubates. The initial and final pH values of the AS/Cys incubates were (A) 3.90 and 4.57, (B) 4.73 and 7.27, and (C) 7.32 and 7.79. (D) Control containing Cys only at an initial pH of 5.43 and a final pH of 5.15. Experimental conditions: The incubates were prepared as described in Figure 2, and the final pH values are those measured after 30 min incubation at room temperature. For MS analysis, the incubates were diluted 10-fold into 50% acetonitrile/0.2% formic acid and directly infused at a flow rate of 1 μL/min into the Z-spray ion source of the mass spectrometer. The instrumental parameters were as follows: source block temperature, 80 °C; capillary voltage, 3.2 kV; cone voltage, 20 kV; collision voltage, 5 V (no collision gas); ToF, −9.1 kV; MCP, 2.1 kV. The peak at *m*/*z* 282.4 is an impurity present in the 50% acetonitrile/0.2% formic acid blank. RA is the relative abundance of the ions.

stored at −20 °C, and used once thawed to avoid decomposition (*27*). Recombinant human brain calbindin D_{28k} (HCalB) was expressed and purified as reported previously (*32*). Bovine serum albumin (BSA; A 7030), L-cysteine (Cys; $C_3H_7NO_2S$, free base), sodium nitrite, DL-dithiothreitol (DTT), 5,5′-dithiobis(2-nitrobenzoic acid) (DTNB), and *N*-ethylmaleimide (NEM) were purchased from Sigma; rabbit muscle glyceraldehyde-3-phosphate dehydrogenase (GAPDH) and tryspin (modified sequencing grade) were obtained from Roche, and diethylenetriaminepentaacetic acid (DTPA) was from ICN Pharmaceuticals. All solutions were prepared using nanopure water (MilliQ) from a Millipore system.

AS Decomposition vs Time. The half-life of AS decreases with pH (*33*). Following dilution of the alkaline stock into water (pH 5.5), 50 mM Tris-HCl buffer (pH 7.4), and 10 mM NaOH, decomposition of AS was monitored spectrophotometrically over 30 min at room temperature in a 1 cm cuvette on a Beckman DU 800 spectrophotometer. Solvent blanks were subtracted from the sample spectra.

Preparation of Reduced BSA. To reconvert its single free Cys34 to the sulfhydryl form, BSA (20 mg/mL, 0.30 mM) was incubated with 2 mM DTT and 0.1 mM DTPA in water at room temperature for 3 h followed by dialysis (MWCO 12000−14000; SpectroPor) vs 0.1 mM DTPA for 48 h with three buffer changes. The concentration of the resulting BSA solution was determined spectrophotometrically ($\epsilon_{278} = 43.0$ mM^{-1} cm^{-1}) (*34*) on a Beckman DU 650 spectrophotometer. DTNB titration ($\epsilon_{412} = 13.6$ mM^{-1} cm^{-1}) (*35*) revealed that the free sulfhydryl content increased from ∼0.3 to 0.9 per BSA molecule following incubation with DTT. Stock solutions of reduced BSA were stored in 0.1 mM DTPA at −80 °C prior to use.

Preparation of GAPDH and HCalB Stock Solutions. An ammonium sulfate suspension (10 mg/mL) of GAPDH was diluted 2-fold with water and dialyzed (MWCO 6000−8000; Spectrum) vs water for 3 h, followed by three changes of 50 mM Tris-HCl buffer (pH 7.4) over 48 h. The GAPDH concentration was determined spectrophotometrically (ϵ_{280} = 149 mM^{-1} cm^{-1} per monomer) (*36*) and its free sulfhydryl content measured by DTNB titration. Stock solutions were stored at −80 °C.

HCalB stocks were stored in 20 mM Tris-HCl buffer (pH 7.4) containing 1 mM $CaCl_2$ and 5 mM β-mercaptoethanol at −80 °C. Mercaptoethanol and excess Ca were removed immediately prior to use by centrifugal ultrafiltration (Ultrafree 0.5 centrifugal filters; Millipore). The volume of the

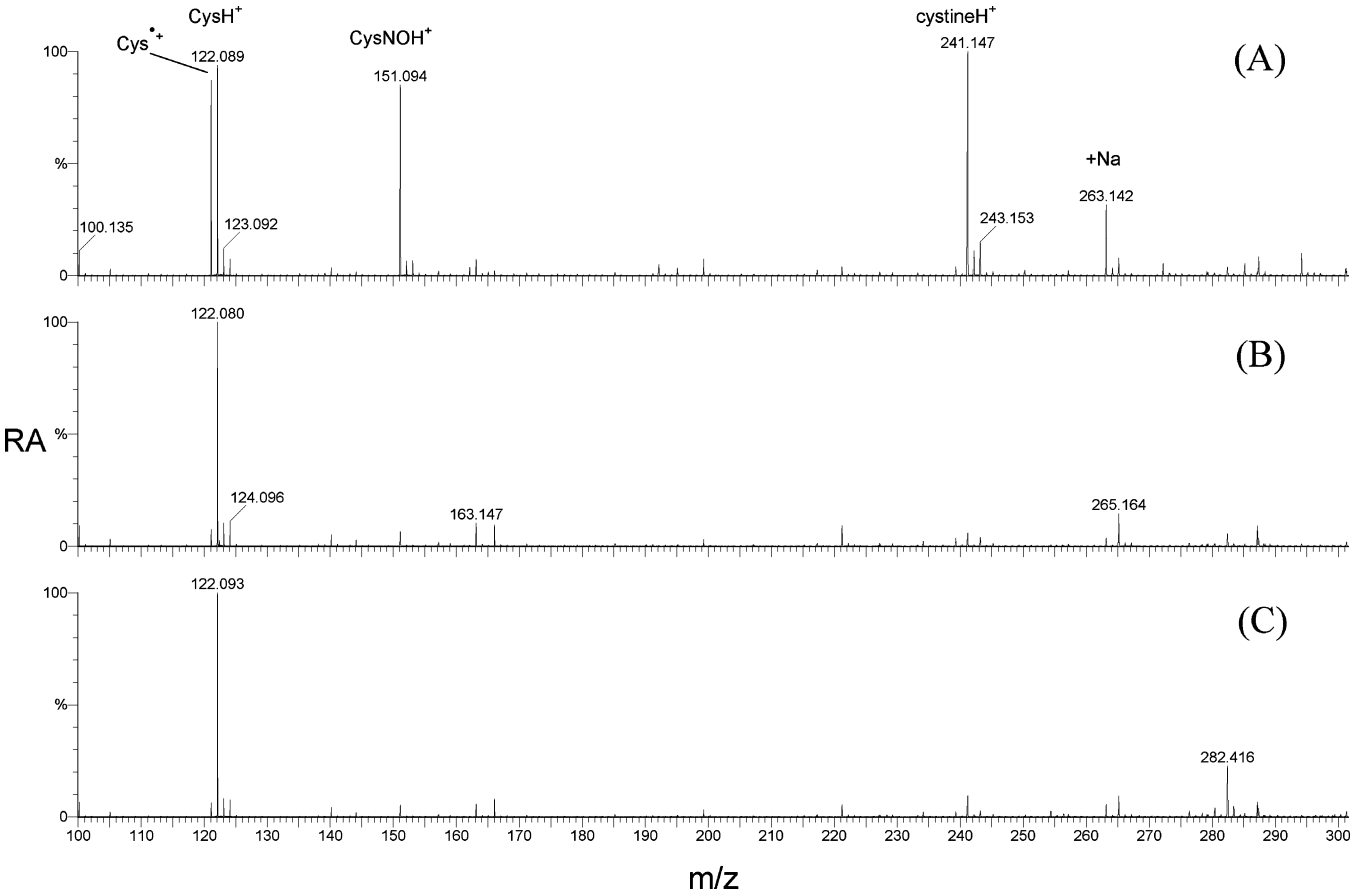

FIGURE 4: Effects of pH on the ESI mass spectra of 30 min $NaNO_2$/Cys incubates. The initial and final pHs of the $NaNO_2$/Cys incubates were (A) 3.42 and 4.05, (B) 7.36 and 7.14, and (C) 7.81 and 7.84. The experimental conditions are given in Figure 3.

stock was twice reduced by ~20-fold over 30 min at 4 °C, and the HCalB concentration was measured spectrophotometrically (ϵ_{280} = 28.0 mM^{-1} cm^{-1}) (*37*).

AS/Cys and AS/Protein Incubates. Freshly prepared stock solutions of Cys in water (pH 5.43) and AS in 10 mM NaOH were mixed at room temperature to give a 15 mM amount of each reagent. The pH of the mixture (9.57) was adjusted with 1 N HCl and monitored at 10 min intervals using an Orion Model 9810BN micro pH electrode (Thermo Electron Corp.). Control incubates containing 15 mM Cys and 15 mM $NaNO_2$ also were examined. HCalB and GAPDH were incubated with AS, NEM, Cys, or $NaNO_2$ in Tris-HCl buffer (pH 7.4) at room temperature for 10−60 min and the products analyzed by ESI-MS. The BSA incubates were prepared in water since buffer salts interfered with the ESI-MS analysis of this protein.

Tryptic Digestion of GAPDH. Untreated and modified GAPDH was diluted to 2 mg/mL and digested at a GAPDH monomer to trypsin ratio of 20:1 (w/w) at 37 °C for 3 h in 50 mM Tris-HCl buffer. Digestion was quenched by freezing at −80 °C.

Mass Spectrometric Analyses. The incubates and protein digests were diluted 10−50-fold into 50% acetonitrile/0.2% formic acid or 20% methanol/5% acetic acid. ESI-MS and MS/MS analysis was carried out on a Waters Micromass Q-ToF2 mass spectrometer operating in the positive ion mode following direct infusion of the samples into the Z-spray ion source. The instrumental parameters are listed in the figure legends. Data analysis and deconvolution were performed using MassLynx 4.0 software (Waters Micromass). Mass calibration was carried out using human [Glu^1]-fibrinopeptide B, and the mass accuracy of the instrument was ~60 ppm. Thus, mass shifts of ±2 units for HCalB (30306 units) and the GAPDH monomer (35692 units) and ±4 units for BSA (66430 units) are within the expected experimental error.

RESULTS

Decomposition of AS. The absorbance maximum of AS shifts from 250 nm at pH >11 to 237 mm at pH <10 (*3*, *27*). The decay of the 237 nm absorption band (Figure 1) reveals a half-life of 5 min for the salt at pH 5.5 (water) and 7.4 (50 mM Tris-HCl buffer) at 22 °C. This is similar to the literature (*27*) half-life of 4.4 min at pH 7.4 (phosphate-buffered saline) and 37 °C. As reported previously (*27*), AS undergoes slow decomposition in 10 mM NaOH since its 250 nm absorption band dominates the spectrum even after 30 min (Figure 1C).

Reactions in the AS/Cys Incubates. The pH of the AS/Cys and $NaNO_2$/Cys incubates in water was monitored using a micro pH electrode at 10 min intervals (Figure 2). Hydroxylamine, formed on conversion of the *N*-hydroxysulfenamide to the disulfide, will consume protons at low pH ($OHNH_3^+ \rightarrow OHNH_2 + H^+$, $pK_a = 5.96$), but no solution pH changes are predicted on sulfinamide formation since both OH^- and H^+ are released (Scheme 1). At pH <4, AS ($H_2N_2O_3 \rightarrow 2NO + H_2O$) releases NO but no HNO (*33*), and the AS/Cys incubate with an initial pH of 3.9 undergoes a small pH increase ($\Delta pH = 0.67$) over 30 min similar to the pH 3.42 $NaNO_2$/Cys incubate (Figure 2). Thus, S-

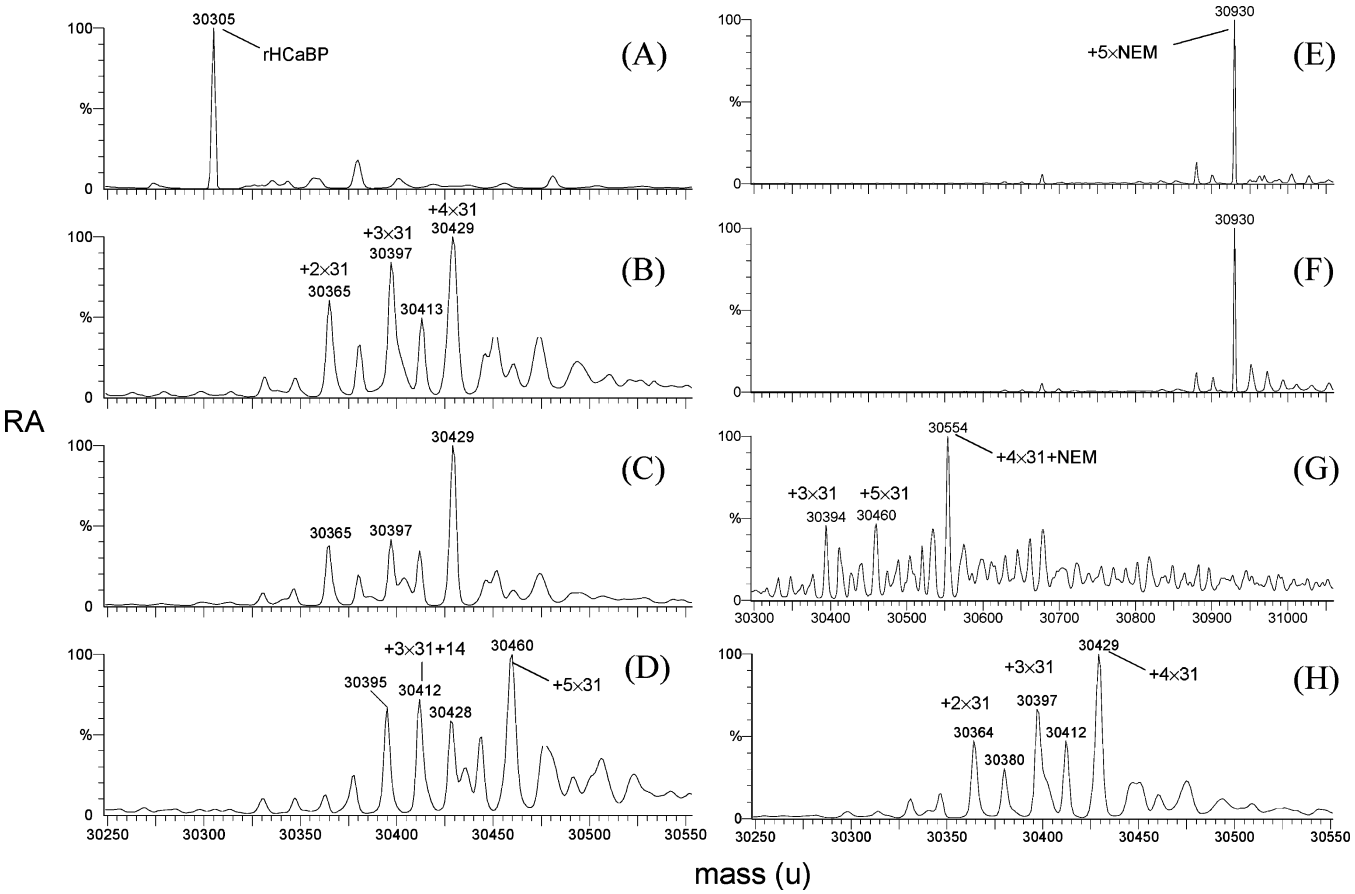

FIGURE 5: Time dependence and confirmation (using NEM) of thiol modification in the AS/HCalB incubates. Deconvolved ESI mass spectrum of (A) untreated HCalB, (B) 10 min AS/HCalB incubate, (C) 25 min AS/HCalB incubate, (D) 60 min AS/HCalB incubate, (E) 30 min NEM/HCalB incubate, (F) 30 min NEM/HCalB incubate following further incubation with AS for 25 min, (G) 25 min AS/HCalB incubate following further incubation with NEM for 30 min, and (H) 25 min AS/HCalB incubate with DTPA. Experimental conditions: 2-Mercaptoethanol-free HCalB (150 μM) was added to 1.5 mM AS, 1.5 mM NEM, and 0.1 mM DTPA (where indicated) in 20 mM Tris-HCl buffer (pH 7.4) at room temperature. Incubates were diluted 25-fold into 50% acetonitrile/0.2% formic acid and directly infused at a flow rate of 1 μL/min into the Z-spray ion source of the mass spectrometer. The instrumental parameters were as follows: source block temperature, 80 °C; capillary voltage, 3.3 kV; cone voltage, 45 V; collision voltage, 10 V (5.5×10^{-5} Torr collision gas); ToF, −9.1 kV; MCP, 2.1 kV. RA is the relative abundance of the ions.

nitrosation of Cys likely occurs in both incubates below pH 4:

$$\mathrm{Cys} + \mathrm{HNO_2} \rightarrow \mathrm{CysNO} + \mathrm{H_2O} \qquad (2)$$

Acidic solutions of HNO_2 react via N_2O_3 or NO^+ intermediates depending on the pH and other variables (*38*).

The large ΔpH increase (+2.5) over 30 min in the pH 4.73 AS/Cys incubate signals that as AS decomposes, Cys is converted to cystine with release of NH_2OH (Scheme 1) below its pK_a. The relatively small pH increases in the pH 6.76 and 7.32 AS/Cys incubates (Figure 2A) are consistent with disulfide and/or sulfinamide formation since NH_2OH remains largely deprotonated at these higher pH values. No reaction is expected in the pH 7.36 or 7.81 $NaNO_2$/Cys incubates because NO_2^- is a weak nitrosating agent in basic media (*38*).

The AS/Cys incubates were examined by ESI-MS after 30 min since the decomposition of the salt is complete within this time period at pH 4−8 (Figure 1A,B). Peaks at *m*/*z* 241, 263, and 285 in the high-mass region of the spectra (Figure 3A−C) are assigned to the MH^+, MNa^+, and $(M - H + 2Na)^+$ ions arising from protonated and sodiated forms of the disulfide, cystine. Formation of cystine was confirmed by fragmentation of the MH^+ ion at *m*/*z* 241, which yielded a MS/MS spectrum with fragment ions at *m*/*z* 224, 195, 158, 152, 122, and 120 as reported previously (*39*). In contrast, a prominent single peak at *m*/*z* 243, assigned to the MH^+ ion of the noncovalent Cys dimer (Cys_2), appears in the high-mass region of the Cys-only spectrum (Figure 3D). Sodiated Cys_2 ions are of low abundance since the free base form of Cys ($C_3H_7NO_2S$) was used and the Cys-only solution contained no added sodium salts such as AS ($Na_2N_2O_3$).

The MH^+ of Cys (*m*/*z* 122) dominates the low-mass range of the Cys-only spectrum (Figure 3D). This ion also is present in spectrum C but not in spectrum B, indicating that Cys was fully oxidized in the pH 4.73 AS/Cys incubate. The NO released from AS at pH <4 (*33*) will react with O_2 to yield a number of S-nitrosating agents including HNO_2 (*40*). $CysNOH^+$ (*m*/*z* 151) and $Cys^{\bullet+}$ (*m*/*z* 121) ions, which are indicative of CysNO formation (*41*), are clearly visible in the spectrum of the pH 3.90 AS/Cys incubate (Figure 3A). The odd-electron $Cys^{\bullet+}$ ions arise from protonation of the cysteinyl radicals $(Cys\text{-}H)^\bullet$ formed on CysNO homolysis in the ESI source (*41*):

$$\mathrm{CysNO} \rightarrow (\mathrm{Cys\text{-}H})^\bullet + \mathrm{NO}^\bullet \qquad (3)$$

The cystineH^+ peak (*m*/*z* 241) in this spectrum is assumed

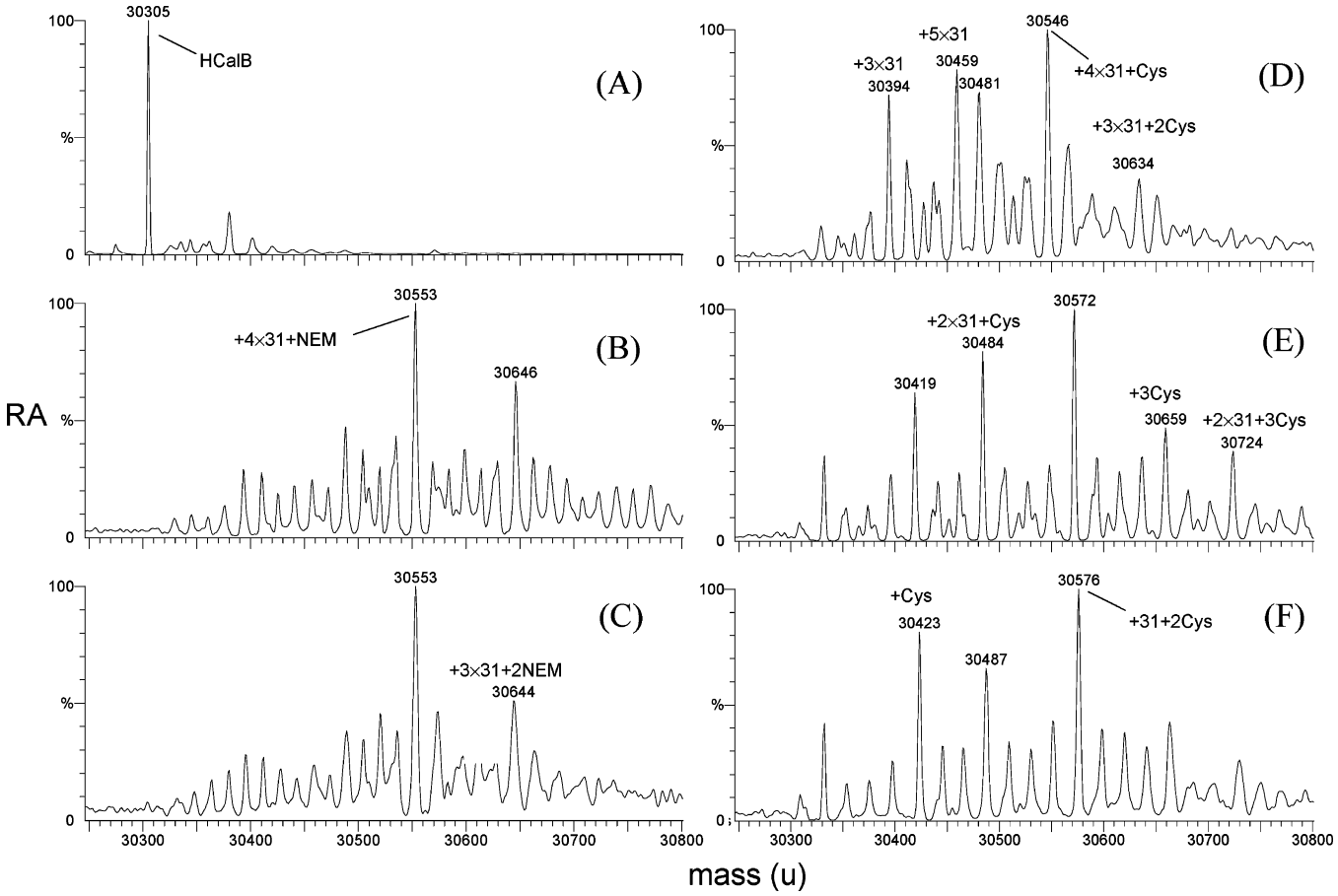

FIGURE 6: AS promotes mixed disulfide formation between HCalB and free Cys. Deconvolved ESI mass spectrum of (A) 25 min Cys/HCalB incubate, (B) 10 min AS/HCalB incubate following further incubation with NEM for 15 min, (C) 10 min AS/HCalB incubate following further incubation with NEM for 15 min and then Cys for 40 min, (D) 25 min AS/HCalB incubate following further incubation with Cys for 50 min, (E) 60 min AS/Cys/HCalB incubate, and (F) 60 min AS/Cys/HCalB incubate following further incubation with 6 mM NEM for 30 min. Experimental conditions: The free Cys concentration was 1.5 mM in (A), 7.5 mM in (C), and 0.75 mM elsewhere. The AS concentration was 3 mM in (E) and (F) and 1.5 mM elsewhere. Unless indicated, the concentrations of the other reagents are given in Figure 5 as are the MS procedures used for the analyses.

to arise partly from $(Cys\text{-}H)^{\bullet}$ dimerization [$(Cys\text{-}H)^{\bullet} + (Cys\text{-}H)^{\bullet} \rightarrow$ cystine] in the ESI source since AS does not liberate HNO at pH <4.0 (*33*) to generate the disulfide via Scheme 1. Thus, from the spectra in Figure 3, we conclude that the HNO produced on AS decay combines rapidly with free Cys to form the *N*-hydroxysulfenamide, which reacts with a second Cys to yield cystine. At pH <4, CysNO is formed following NO release from AS.

The ESI mass spectra of the $NaNO_2$/Cys incubates (Figure 4) support these conclusions. The pH 7.81 and 7.36 incubates yield spectra that are dominated by the $CysH^+$ ion (*m*/*z* 122) as seen in the spectrum of Cys alone (Figure 4B,C vs Figure 3D), which was expected since NO_2^- is not an effective S-nitrosating agent at neutral pH (*38*). The spectra of the pH 3.42 $NaNO_2$/Cys and pH 3.90 AS/Cys incubates are essentially identical (Figures 4A and 3A) and contain the $Cys^{\bullet+}$ ion (*m*/*z* 121), confirming that CysNO is formed in both incubates at low pH. Since S-nitrosation by HNO_2 (eq 2) is quantitative at low pH (*38*), the $CysH^+$ ion (*m*/*z* 122) likely arises from reductive cleavage of CysNO in solution, which is catalyzed by copper impurities (*41*) present at the 1−2 μM level in the buffers (*42*). This process would also increase the cystine concentration in solution since Cys is oxidized during redox turnover of the copper catalyst (*41*). Significantly, no Cys sulfinamide ions (*m*/*z* 153, M + 31) were detected in the spectra of the AS/Cys incubates at any pH, revealing that the *N*-hydroxysulfenamide intermediate reacts with a second Cys molecule faster than it releases OH^- (Scheme 1). In summary, incubation of free Cys with AS produces cystine due to reaction with HNO (Scheme 1) at pH 7 and CysNO due to reaction with HNO_2-derived nitrosating agents at pH <4.0. Variation in the AS (200 μM to 15 mM) and Cys (200 μM to 15 mM) concentrations in the incubates at pHs above 5 gave rise to cystine exclusively (data not shown), underscoring the efficiency of this pathway (Scheme 1) when RSH = Cys.

Reactions in the AS/HCalB Incubates. The deconvolved ESI mass spectrum of untreated HCalB (Figure 5A) exhibits a major peak at 30305 ± 1 units in agreement with the average mass predicted from the native HCalB sequence (*43*) plus the three amino acids (GlySerHis) that are added to the N-terminus of HCalB when it is expressed from the pET15b vector (*32*). Incubation with the thiol-specific reagent, NEM (reaction 4) (*19*), was carried out to confirm the number of

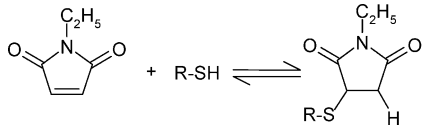

(4)

free thiols in the protein. The mass spectrum of a 30 min

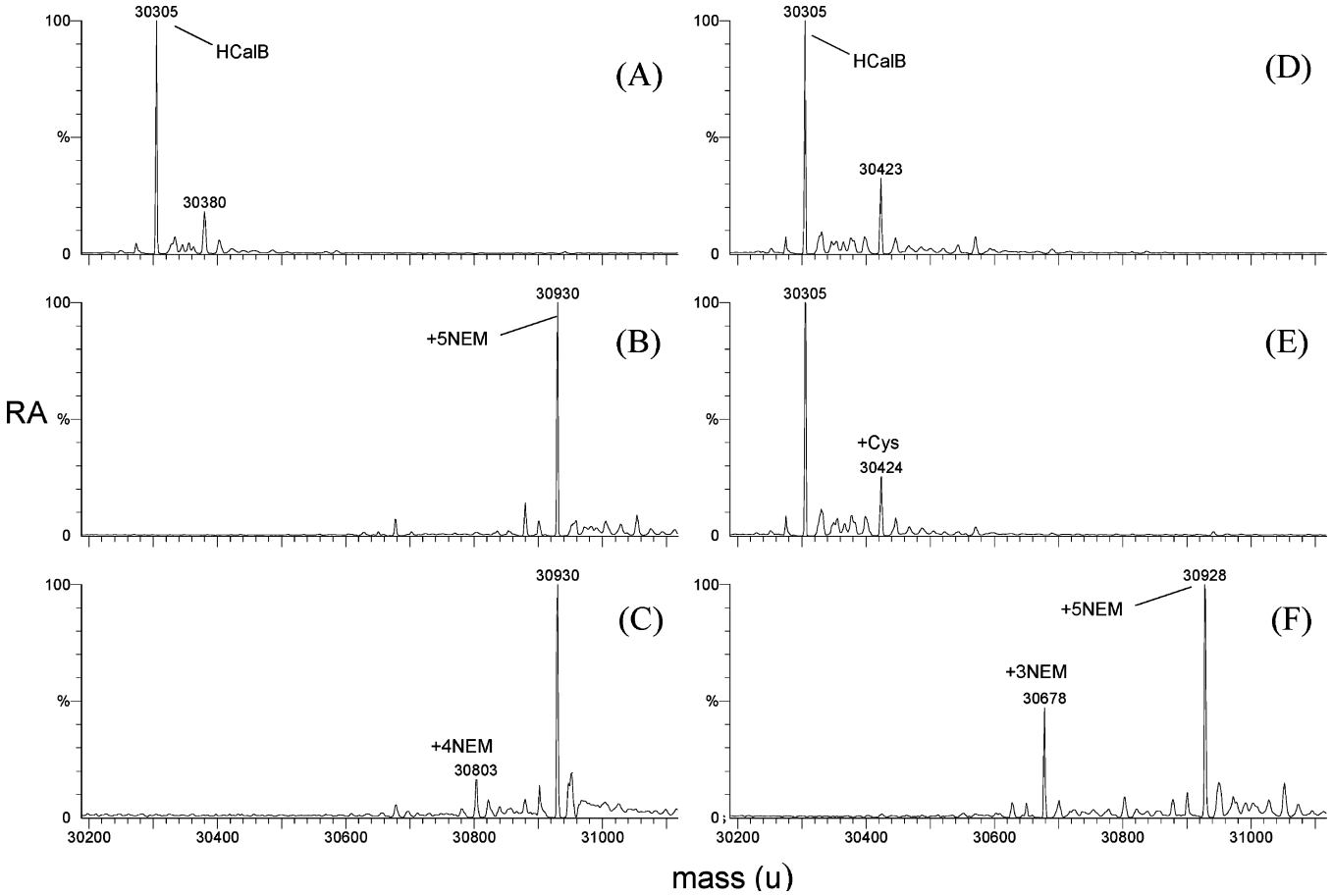

FIGURE 7: Incubation with $NaNO_2$ does not modify HCalB at physiological pH. Deconvolvd ESI mass spectrum of (A) 60 min $NaNO_2$/HCalB incubate, (B) 10 min $NaNO_2$/HCalB incubate following further incubation with NEM for 15 min, (C) 10 min $NaNO_2$/HCalB incubate following further incubation with NEM for 15 min and then free Cys for 40 min, (D) 25 min $NaNO_2$/HCalB incubate following further incubation with free Cys for 50 min, (E) 60 min $NaNO_2$/Cys/HCalB incubate, and (F) 60 min $NaNO_2$/Cys/HCalB incubate following further incubation with 6 mM NEM for 30 min. Experimental conditions: The $NaNO_2$ concentration was 3 mM in (E) and (F) and 1.5 mM elsewhere. The concentrations of the other reagents and the MS procedures are given in Figures 5 and 6. The peak at 30380 units in (A) is assigned to a β-mercaptoethanol adduct of HCalB (M + 78).

NEM/HCalB (10:1) incubate shows a single M + 625 peak (Figure 5E), consistent with the presence of five free sulfhydryls (125 units per NEM label) in HCalB (*19*).

The spectrum of the 10 min AS/HCalB incubate reveals that no unmodified protein was present and the protein mass increased further with the incubation time (Figure 5B−D). Peaks at 30365 ± 2, 30397 ± 1, 30429, and 30460 units define a M + n × 31 series, with the M + 124 ($n = 4$) and M + 155 ($n = 5$) peaks dominant in spectra of the 25 and 60 min incubates, respectively. The M + n × 31 adducts are attributed to the HNO-induced conversion of the free thiols in HCalB to sulfinamides ($RSONH_2$) (Scheme 1) in the AS incubates. The presence of a second M + 14 + n × 31 series, including the M + 14 + 3 × 31 peak at *m*/*z* 30412 units (Figure 5D), reveals that HNO also induces formation of M + 14 adducts in HCalB, which are discussed below (see Discussion).

The mass spectrum of the $NaNO_2$/HCalB incubate is almost identical to that of the untreated protein (Figure 7A vs Figure 5A), confirming that HCalB is modified at pH 7.4 by HNO and not NO_2^-. Since trace copper catalyzes protein S-nitrosation (*44*, *45*), the effect of the copper chelator DTPA (*46*, *47*) was examined. There are no detectable differences with and without DTPA in the spectra of the 25 min (Figure 5H vs Figure 5C) or 60 min (data not shown) AS/HCalB incubates, suggesting that HNO-induced modification is not metal-catalyzed. Similarly, the spectra of the 60 min $NaNO_2$/HCalB (Figure 7A) and 60 min $NaNO_2$/DTPA/HCalB (data not shown) incubates are the same so trace metal does not promote modification of HCalB by $NaNO_2$ at pH 7.4.

Blockage of its Cys residues by preincubation with NEM (reaction 4) prevents HCalB modification on subsequent incubation with AS. Since the resultant spectrum (Figure 5F) is identical to that of the NEM-only incubate (Figure 5E), the Cys residues in HCalB are clearly targeted by HNO and not lysine residues although amines also are reported to be reactive with HNO (*4*). As expected, preincubation with AS largely prevented NEM modification since only singly NEM-modified HCalB was detected (Figure 5G), providing further evidence that HNO targets the protein's Cys residues.

As predicted by Scheme 1 and as seen for free Cys (Figure 3), HNO can induce disulfide formation. Since free thiols are abundant in cells, a 5-fold excess of free Cys was added to a 25 min AS/HCalB incubate. The mass spectrum, recorded after a further 50 min incubation (Figure 6D), contains peaks at 30546 units (M + 4 × 31 + 119) and 30634 units (M + 3 × 31 + 2 × 119) assigned to singly and doubly Cys-labeled HCalB, respectively. Addition of free Cys to the $NaNO_2$/HCalB control also led to Cys labeling as seen from the M + 119 peak at 30423 ± 1 unit (Figure

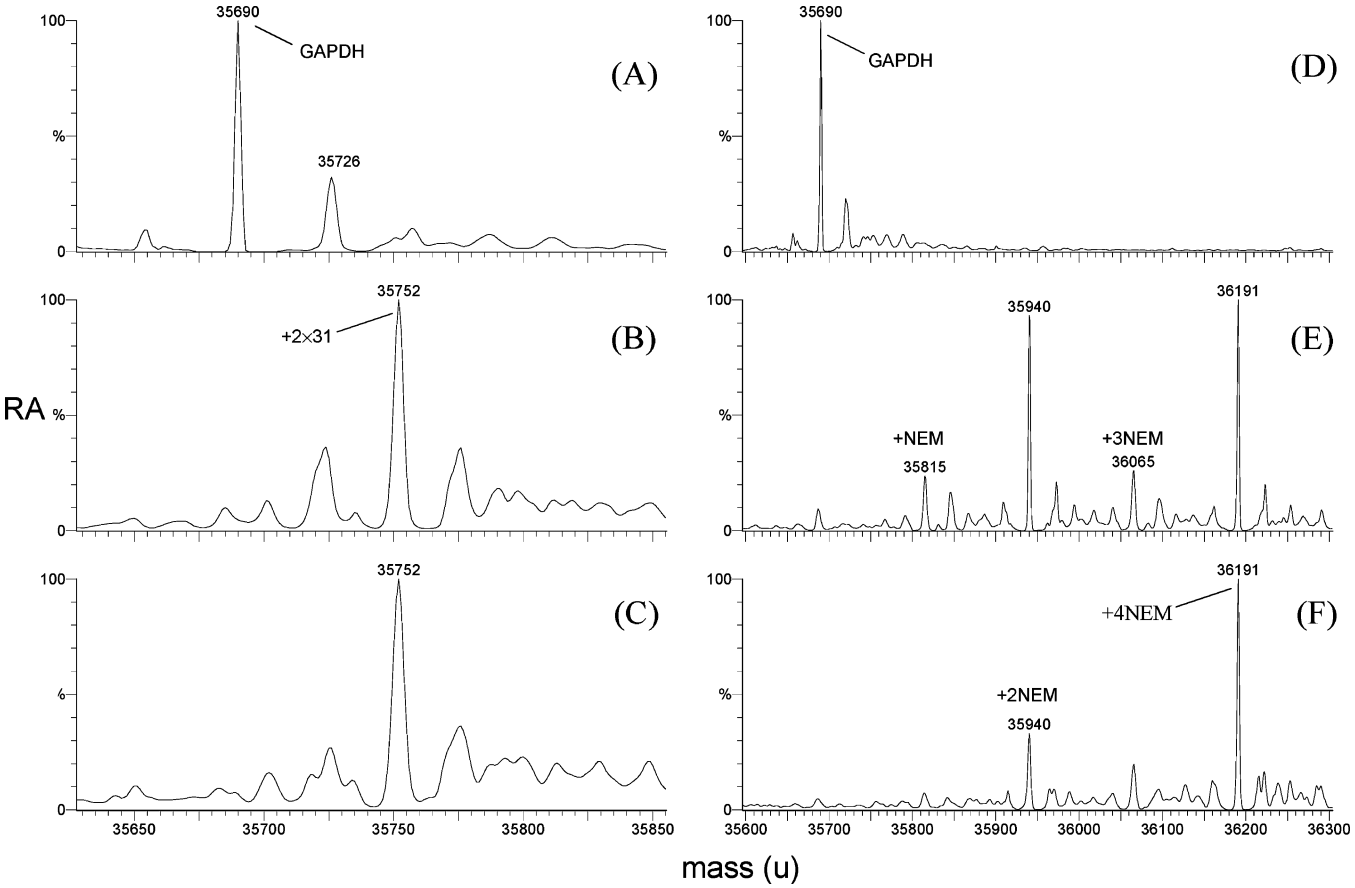

FIGURE 8: Time dependence and confirmation (using NEM) of thiol modification in AS/GAPDH incubates. Deconvolved ESI mass spectrum of (A) untreated GAPDH, (B) 25 min AS/GAPDH incubate, (C) 60 min AS/GAPDH incubate, (D) 60 min $NaNO_2$/GAPDH incubate, (E) 30 min NEM/GAPDH incubate, and (F) 30 min NEM/GAPDH following further incubation with AS for 30 min. Experimental conditions: GAPDH (120 μM), 2.4 mM AS, 2.4 mM $NaNO_2$, and 2.4 mM NEM (where indicated) were incubated in 50 mM Tris-HCl buffer (pH 7.4) at room temperature. The MS procedures are given in Figure 5.

7D) that is not present in the spectrum of the Cys/HCalB incubate (Figure 6A). Thus, Cys labeling of HCalB may be initiated by S-nitrosation of free Cys by HNO_2 (eq 2) following 25-fold dilution of the incubates into the MS analysis solution (50% acetonitrile/0.2% formic acid, pH 2.7). Cysteinyl radicals $(Cys\text{-}H)^{\bullet}$ formed in the ESI source (eq 3) can react with free sulfhydryl groups in HCalB. If the latter are blocked with NEM prior to Cys addition and acidification, peaks due to NEM ($M + m \times 125 + n \times 31$ or $M + m \times 125$) but not Cys labeling ($M + m \times 119 + n \times 31$ or $M + m \times 119$) are observed in the spectra of the AS/HCalB and $NaNO_2$/HCalB incubates (Figure 6C vs Figure 6D; Figure 7C vs Figure 7D).

To determine whether Cys labeling could compete with $RSONH_2$ formation if the thiol were present when the RSNHOH intermediate was formed, 150 μM HCalB was added to a solution of 3 mM AS and 0.75 mM free Cys. The mass spectrum recorded after 60 min incubation exhibits prominent peaks at $M + n \times 31 + m \times 119$ ($n = 0-2$, $m = 1-3$) (Figure 6E) due to Cys labeling. The subsequent addition of NEM had no effect on the mass spectrum (Figure 6F vs Figure 6E), revealing that Cys labeling of HCalB involved S-cysteinylation or mixed disulfide formation. $NaNO_2$ plus Cys did not modify HCalB under the same conditions since only NEM derivatives were detected in the mass spectrum when the thiols were blocked prior to acidification (Figure 7F vs Figure 7E). Thus, S-cysteinylation in the AS/Cys/HCalB incubates is HNO-induced, but free Cys must be present in solution when the RSNHOH is generated, indicating that this intermediate is readily converted to $RSONH_2$ (Scheme 1). In summary, three HNO-mediated modifications can be deduced from the mass spectral analysis of intact HCalB: conversion of its free sulfhydryls to sufinamides, to $M + 14$ derivatives (see Discussion), and to mixed disulfides in the presence of free Cys.

Reactions in the AS/GAPDH Incubates. The deconvolved ESI mass spectrum of untreated GAPDH shows a major peak at 35690 units, in agreement with the theoretical average subunit mass of 35692 units, and a less intense peak at 35726 units tentatively assigned to oxidized ($M + 32$) protein (Figure 8A). The domination of the spectra by an $M + 2 \times 31$ peak at 35752 units following 25 or 60 min incubation with AS (Figure 8B,C) reveals that each subunit is labeled with two $RSONH_2$ groups. The weaker peak at 35776, which is not present in the untreated protein, may be a sodiated form ($M + 2 \times 31 + 23$). HNO is the modifying reagent since the spectrum of the $NaNO_2$/GAPDH control is similar to that of untreated GAPDH (Figure 8A vs Figure 8D), and preincubation with NEM inhibited the HNO-induced conversion to $RSONH_2$ of two Cys residues in the GAPDH monomer (Figure 8F). However, DNTB titration (Table 1) reveals only 0.56 ± 0.27 free thiol per monomer in AS-treated GAPDH compared to 1.22 ± 0.10 in the NEM-treated protein. The mass spectrum of the NEM/GAPDH incubate exhibits major peaks at 35940 and 36191 units (Figure 8E), corresponding to NEM-labeled monomer at two ($M + 2 \times$

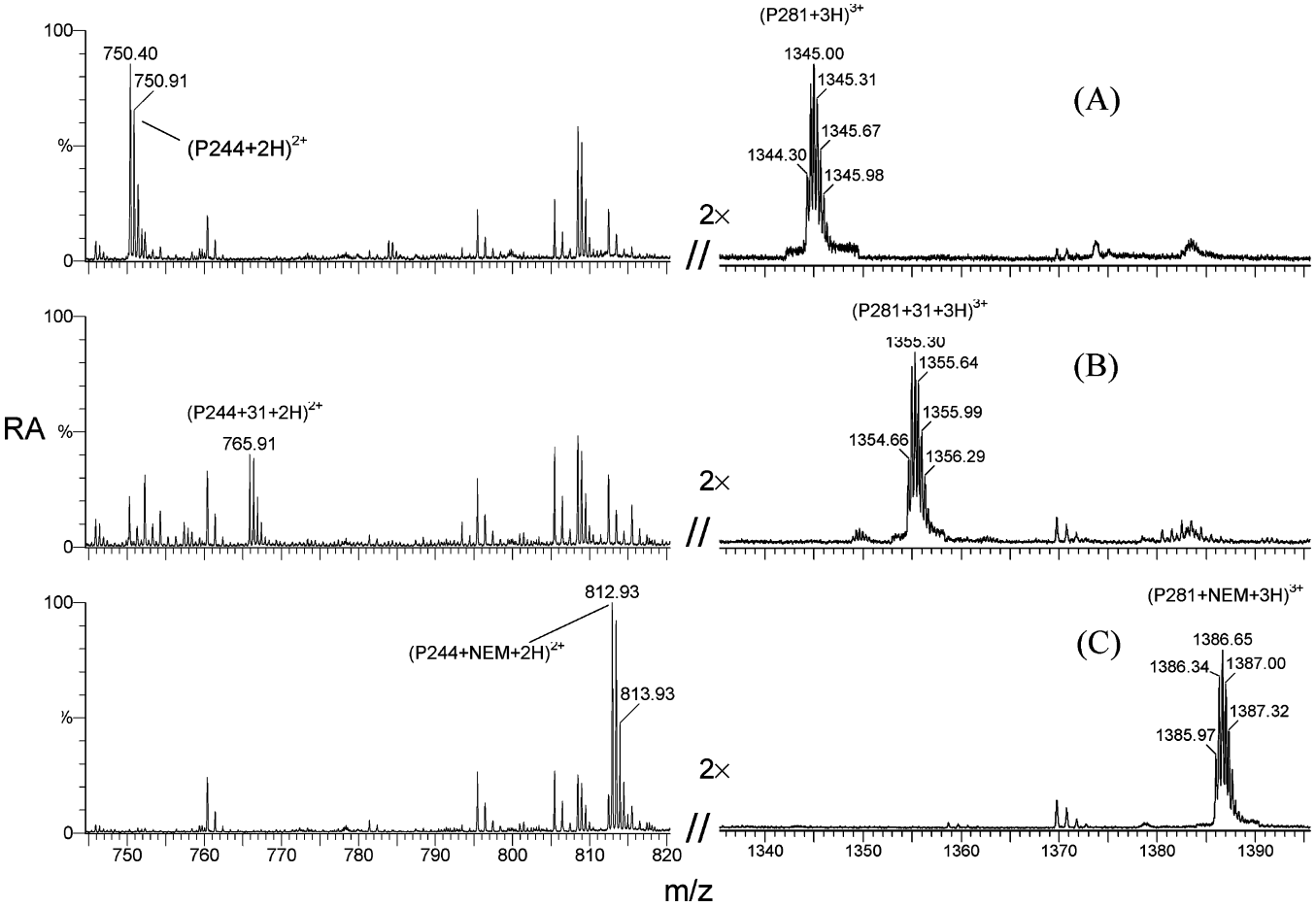

FIGURE 9: ESI mass spectra of tryptic peptides V232−K245 (P244) and G269−K306 (P281) of GAPDH. Observed ESI mass spectrum in the *m*/*z* 600−800 and *m*/*z* 1200−1400 ranges of the tryptic digests of (A) untreated GAPDH, (B) 25 min AS/GAPDH incubate, and (C) 30 min NEM/GAPDH incubate. Experimental procedures: Protein from the incubates in Figure 8 was digested as described under Materials and Methods, and the digests were diluted 50-fold into 50% acetonitrile/0.2% formic acid. The MS parameters are listed in Figure 5. As indicated on the spectra, the peak intensities in the *m*/*z* 1200−1400 range were expanded 2-fold.

Table 1: DTNB Titration of the Free Thiols in GAPDH Following Incubation with AS and NEM[a]

	untreated GAPDH	AS-treated GAPDH	NEM-treated GAPDH
thiol/monomer[b] (mol/mol)	4.01 ± 0.28	0.56 ± 0.27	1.22 ± 0.10

[a] GAPDH (120 μM) was incubated with 2.4 mM AS for 25 min and 2.4 mM NEM for 30 min in 50 mM Tris-HCl buffer (pH 7.4) at room temperature. The number of free thiols in untreated, AS-treated, and NEM-treated GAPDH was determined by DTNB titration (ϵ_{412} = 13.6 mM^{-1} cm^{-1}). [b] GAPDH from four different controls (no reagent) and AS and NEM incubates were titrated with DTNB. The average number of free thiols per GAPDH monomer and the standard deviations are given.

Table 2: Monoisotopic Masses of y Ions in the MS/MS Spectra of GAPDH Tryptic Peptides P244 and P149/153[a]

	P244 y ions				P149/153 y ions		
		obsd				obsd	
ions	calcd	native	NEM	AS	calcd	native/AS	NEM
1	175	175	175	175	147	147	147
2	278	278	403	244	218	218	218
3	379	379			331		
4	492	492	617	458	428	428	428
5	607	607	732	573	499	499	499
6	706	706	831	672	612	612	612
7	806	806	931	772	716		
8	893	893	1018	859	830		
9	992	992	1117	958	931		1056
10	1106	1106	1231		1032		1157
11	1203	1203	1328	1169	1135	1133	1385
12	1304	1304	1429	1270	1222	1220	1472
13	1401	1401	1526	1367	1293		
14	1499	1500	1625	1466	1407	1405	
15					1494	1492	1744
16					1594		
17					11706	1704	1956

[a] The ions at *m*/*z* 750.40 (Figure 9A), 765.91 (Figure 9B), 812.93 (Figure 9C), 852.45 (Figure 10A), and 978.50 (Figure 10D) were selected in the quadrupole and subjected to CID (25−35 V), and the product ions were analyzed by ToF.

125) and four (M + 4 × 125) thiols, respectively, which is consistent with the DTNB titration data (Table 1). HNO-induced intramolecular disulfide formation between Cys149 and Cys153 in addition to conversion of Cys244 and Cys281 to sulfinamides (Scheme 1) would reconcile both the DTNB titration (Table 1) and MS (Figure 8B,C) results obtained for the AS/GAPDH incubates.

The anticipated thiol modifications were confirmed by peptide mass mapping of GAPDH. The MH_2^{2+} ion of tryptic peptide V232−R245 [P244, M_r (monoisotopic) = 1498.79 u] is seen at *m*/*z* 750.40 in the map of native GAPDH and at M + 31 and M + 125 in the maps of the AS- and NEM-treated protein (Figure 9), indicating Cys244 oxidation to the sulfinamide (Scheme 1) and alkylation (reaction 4), respectively. The mass increase of +125 in the y fragment

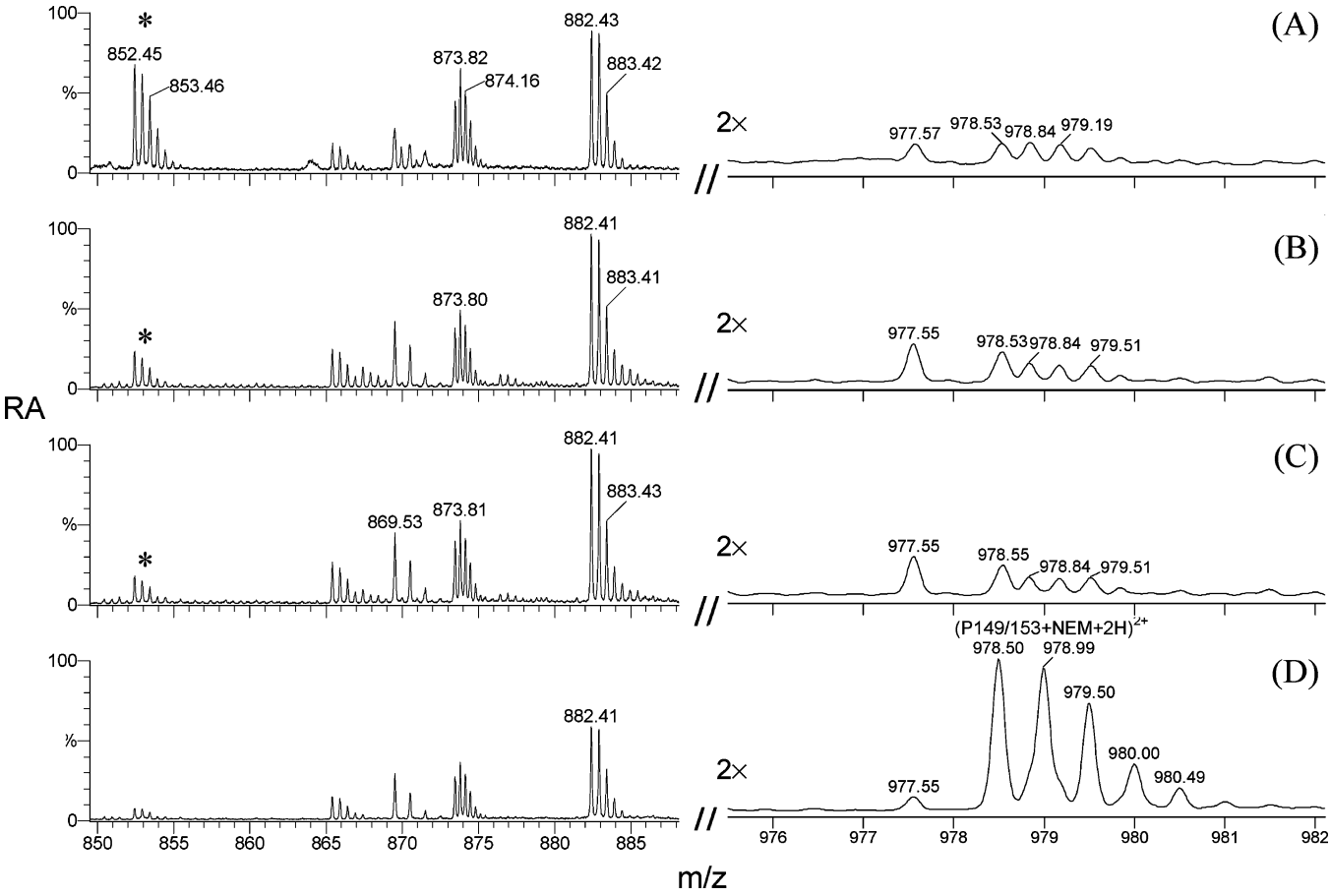

FIGURE 10: ESI mass spectra of tryptic peptide I143−K159 (P149/153) of GAPDH. Observed ESI mass spectrum in the *m*/*z* 850−900 and *m*/*z* 976−982 ranges of the tryptic digests of (A) untreated GAPDH, (B) 25 min AS/GAPDH incubate, (C) 25 min AS/GAPDH following further incubation with NEM for 30 min, and (D) 30 min NEM/GAPDH incubate. The experimental procedures are given in Figure 9. Peaks corresponding to the doubly protonated $(M - 2)H_2^{2+}$ ion of peptide P149/153 that contain a Cys149-Cys153 disulfide are indicated by an asterisk (*). As indicated on the spectra, the peak intensities in the *m*/*z* 976−982 range were expanded 2-fold.

ions, except for y1, in the MS/MS spectrum of NEM-modified P244 (Table 2) is consistent with alkylation of the penultimate residue, Cys244. The MS/MS spectrum of AS-modified P244 contains y ions, with the exception of y1, that are 34 units lower in mass than the control (Table 2). This is attributed to loss of the sulfinamide group from Cys244 (M + 31 − 65 = M − 34) under the MS/MS conditions. The corresponding modifications of Cys281 can be inferred from the mass increases observed for the MH_3^{3+} ion at *m*/*z* 1344.30 of tryptic peptide G269−K306 [P281; M_r (monoisotopic) = 4029.84 units] (Figure 9). Due to its large size (39 residues), MS/MS analysis of P281 did not lead to sufficient cleavage to confirm Cys281 as the site of modification, but no other residues in P281 (GILGYTEDQVVSCDFNSDTHSSTFDAGAGIALNDHFVK) are expected to exhibit NEM and AS reactivity under the experimental conditions used. Thus, Cys244 and Cys281 are assumed to be converted to sulfinamides in the AS/GAPDH incubates.

A peak at *m*/*z* 852.45 in the peptide map of untreated (Figure 10A,B) and AS-treated GAPDH is assigned to the MH_2^{2+} ion of tryptic peptide I143−K159 [P149/153; M_r (monoisotopic) = 1704.86 units] with an intramolecular disulfide bridge (M − 2). MS/MS analysis reveals that the y11−y16 fragment ions are 2 units lighter than predicted (Table 2). Since Cys149 and Cys153 reportedly form a disulfide in the denatured protein (*48*), the free thiols were blocked with NEM prior to tryptic digestion. The MH_2^{2+} ion at *m*/*z* 978.5 with an isotope separation of 0.5 unit dominates the map of NEM-treated GAPDH (Figure 10D) and is assigned to the doubly NEM-labeled peptide P149/153 (M + 2 × 125). The y11−y16 fragment ions are doubly NEM-labeled whereas y9 and y10 are singly NEM-labeled (Table 2) in the MS/MS spectrum of the 978.5 ion, confirming that residues 7 (Cys149) and 10 (Cys153) undergo alkylation in P149/153.

The weak peak at *m*/*z* 978.5 in Figure 10A−C exhibits the isotopic pattern of a triply charged ion (MH_3^{3+}) with an isotope separation of 0.333 mass unit. Thus, the isobaric (*m*/*z* 978.5) MH_3^{3+} (Figure 10A−C) and MH_2^{2+} (Figure 10D) ions do not arise from the same peptide, which was confirmed by MS/MS analysis (data not shown). HNO must have induced C149−Cys153 disulfide formation *before* NEM was added to the AS/GAPDH incubate (Figure 10C) since the MH_2^{2+} ion at *m*/*z* 978.5, assigned to NEM-labeled P149/153, is absent from the peptide map of this sample. Significantly, no ions corresponding to M + 31 or M + 2 × 31 adducts of P149/153 are seen in the map of AS-treated GAPDH (Figure 10B,C), indicating that neither Cys149 nor Cys153 is converted to $RSONH_2$. (The ions observed between *m*/*z* 865 and 885 can be assigned to native peptides.) In summary, HNO induces intrasubunit disulfide cross-linking between Cys149 and Cys153, and $RSONH_2$ labeling of Cys244 and Cys281 in GAPDH.

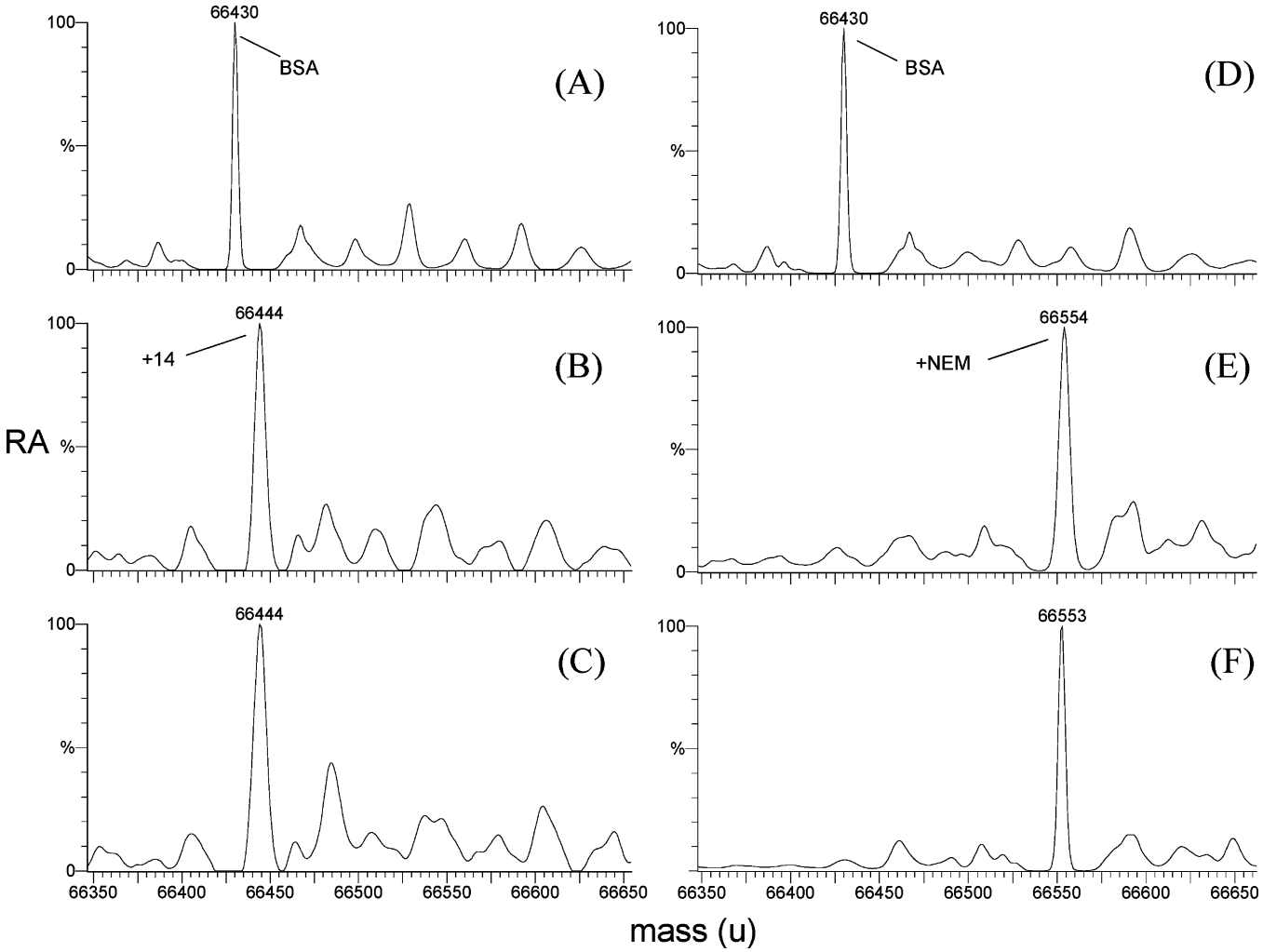

FIGURE 11: Time dependence and confirmation (using NEM) of thiol modification in AS/BSA incubates. Deconvolved ESI mass spectrum of (A) untreated BSA, (B) 25 min AS/BSA incubate, (C) 60 min AS/BSA incubate, (D) 60 min $NaNO_2$/BSA incubate, (E) 30 min NEM/BSA incubate, and (F) 30 min NEM/BSA following further incubation with AS for 30 min. Experimental procedures: BSA (180 μM), 0.9 mM AS, 0.9 mM $NaNO_2$, and 1.8 mM NEM (where indicated) were incubated in water (pH 6.72−7.16) at room temperature. Use of Tris-HCl or phosphate buffers gave an ESI mass spectrum that could not be deconvolved due to extensive adduct formation between BSA and the buffer salts. The MS procedures are given in Figure 5.

Reactions in the AS/BSA Incubates. Incubation of BSA with AS was carried out in water because the presence of 20 mM buffer ions yields an ESI mass spectrum that is difficult to deconvolute. The initial pH of the unbuffered AS/BSA incubates was 6.72, and the final pH was 7.16. The mass spectrum of untreated BSA shows a major peak at 66430 units (Figure 11A) in agreement with its reported average mass (*49*, *50*). An M + 14 peak is observed at 66444 units in the spectrum of the 25 and 60 min AS/BSA incubates (Figure 11B,C) but not in the spectrum of the $NaNO_2$/BSA control (Figure 11D), which is indistinguishable from that of the untreated protein (Figure 11A). Preincubation of BSA with NEM gave rise to singly NEM-labeled BSA (Figure 11E) and inhibited modification by AS (Figure 11F), demonstrating that the single free sulfhydryl of Cys34 is the site of HNO-induced (M + 14) adduct formation (Figure 11B,C). Since this BSA adduct was stable on standing at room temperature overnight (data not shown), it is unlikely the $RS^+{=}NH$ (M + 14) intermediate proposed in Scheme 1. Instead, it is proposed to arise from intramolecular cross-linking between Cys34 and neighboring Lys or Arg residues, since stable sulfinamide cross-links have been reported recently in other proteins (*51*, *52*). Unfortunately, attempts to locate tryptic peptide G21−K41 containing Cys34 in the peptide map of NEM-modified BSA or a cross-linked peptide containing Cys34 in maps of AS-modified BSA were unsuccessful. However, since preincubation with AS blocks NEM reactivity (data not shown), Cys34 is clearly the site of modification by HNO. Significantly, no M + 31 adducts (Figure 11C) or mixed disulfides with added free Cys (data not shown) are formed in the AS/BSA incubates.

DISCUSSION

Despite the growing recognition of its biological importance (*31*), nitroxyl remains one of the least investigated of the biologically and pharmacologically relevant NO_x. Although AS exposure has been reported to modify thiol proteins in vitro and in vivo (*8*, *14*−*18*, *22*, *53*), characterization of the products has not been carried out. The mass spectral data reported here provide the first systematic analysis of the products formed on the reaction of protein thiols with HNO.

The reaction of free Cys with HNO around physiological pH leads exclusively to the disulfide, cystine. Thus, the *N*-hydroxysulfenamide derivative of Cys reacts with a second

Cys molecule faster than it decays to the $RS^+{=}NH$ cation, which leads to the sulfinamide $RSONH_2$ (Scheme 1). The products formed on the reaction of HNO with protein-based Cys are dictated by the environment and include disulfide formation as seen with free Cys.

HCalB is a calcium-binding protein noted for its abundance and specific distribution in mammalian brain and sensory neurons (*54*, *55*). We have shown previously that the five free sulfhydryls of HCalB are S-nitrosated (*19*) and S-thiolated (*41*). HNO induces partial conversion of the five Cys residues to their $RSONH_2$ derivatives (Figure 5D), indicating that loss of OH^- from the *N*-hydroxysulfenamide intermediates is more rapid than intermolecular attack by a second HCalB-based sulfhydryl (Scheme 1). However, HCalB−Cys mixed disulfides were formed when free Cys was present (Figure 6E), indicating that HNO can induce protein S-thiolation. This reversible protein modification signals oxidative stress (*16*) and has been suggested to serve as a general antioxidant defense mechanism analogous to free radical scavenging (*56*).

GAPDH is active as a glycolytic enzyme in its tetrameric form. It catalyzes the conversion of glyceraldehyde 3-phosphate to 1,3-diphospholycerate in the breakdown of glucose to pyruvic acid, an important pathway of carbohydrate metabolism in most organisms. Each subunit contains four Cys residues (Cys149, Cys153, Cys244, and Cys281) with the active site Cys149 (*57*, *58*) close to Cys153 in a conserved pentapeptide, CTTNC (Figure 12A) (*59*). HNO-induced intrasubunit disulfide formation between Cys149 and Cys153 was detected here by ESI-MS (Figure 10), as well as conversion of Cys244 and Cys281 to $RSONH_2$ groups (Figure 9). Since disulfide cross-linking is reversible and the $RSONH_2$ groups are formed far from the active site (Figure 12), the report that incubation with AS at pH 7.4 and 8.6 irreversibly inhibits GAPDH activity (*16*) is surprising. Without characterizing the modified enzyme, the authors speculated that conversion of the active site Cys149 to a sulfinamide was the cause of irreversible inactivation (*16*), but neither M + 31 nor M + 2 × 31 adducts of peptide P149/153 were detected in the peptide mass map of AS-treated GAPDH (Figure 10). Hence, we speculate that conversion of Cys244 and/or Cys281 to $RSONH_2$ may disrupt the active tetrameric structure of GAPDH (Figure 12B). Given the critical importance of thiol modification in the role of GAPDH (*60*−*63*), the effects of HNO on its oligomeric structure and glycolytic activity are under further investigation. Interestingly, GAPDH has been identified as a major S-thiolated protein during oxidative stress (*64*, *65*), and we have reported that it is readily S-thiolated by glutathione thiosulfinate, a decomposition product of GSNO (*41*).

Serum albumin is the most abundant protein in plasma, and its single free sulfhydryl on Cys34 constitutes the major plasma thiol (*34*, *66*). Cys34 appears to be fully converted to a stable M + 14 mass adduct on incubation of BSA with AS (Figure 11B). The environment of Cys34 in HSA (the structure of BSA is unavailable) can be compared to that of Cys244 and Cys281 in GAPDH since X-ray structures are available for both proteins (Figure 12). Thr83 may sterically hinder sulfinamide formation at Cys34 of HSA, but there is no such hindrance around Cys244 or Cys281 in GAPDH. Cys34 of BSA is surrounded by Lys73, Lys137, Arg81, Arg144, and Arg145 (Figure 12C), and intramolecular nucleophilic attack of an amino group on the *N*-hydroxysulfenamide intermediate could produce a sulfenamide that could be air-oxidized to the sulfinamide (Scheme 2). The addition of oxygen with loss of two hydrogens would give rise to the mass increase of 14 units observed for AS-treated BSA. Nucleophilic attack of a neighboring amino group on a sulfenic acid (RSOH) intermediate reportedly leads to intramolecular sulfinamide cross-linking in other proteins (*51*, *52*, *67*). The M + 14 adducts of HCalB also are assumed to result from intramolecular sulfinamide cross-links, but the cross-linked residues cannot be predicted since the three-dimensional structure of HCalB is unknown.

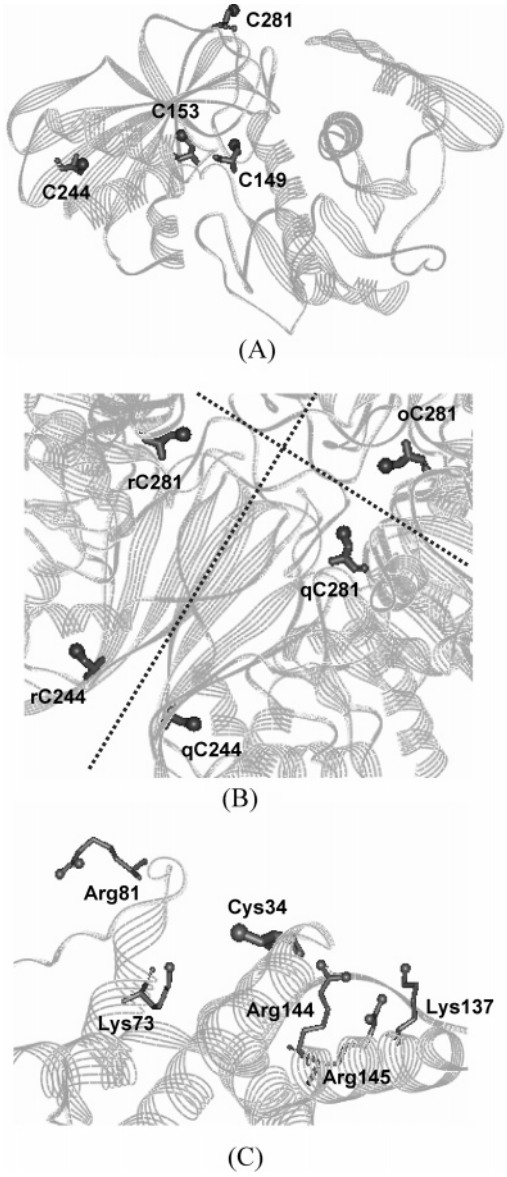

FIGURE 12: Environment of the free sulfhydryl groups in GAPDH and BSA. C_α backbone of GAPDH (PDB code 1JOX) showing the location of (A) the active site C149 and neighboring C153 within each monomer and (B) C244 and C281 relative to the subunit interfaces. The letters o, q, and r correspond to three different subunits of the GAPDH tetramer, and the dashed lines indicate the subunit interfaces. (C) C_α backbone of HSA (PDB code 1HA2) showing the Lys and Arg residues within 14 Å of the protein's single free sulfhydryl on Cys34. The larger balls in the ball-and-stick representation of the Cys side chains represent the sulfur atoms.

Scheme 2

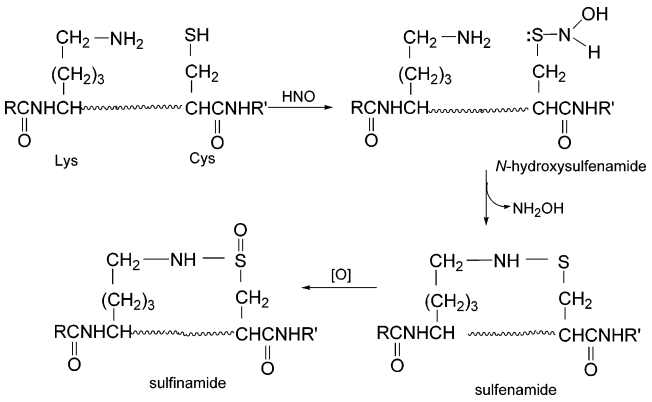

CONCLUSIONS

We provide here the first chemical characterization of protein-based thiol derivatization mediated by AS-derived HNO. This NO_x induces thiol conversion to four distinct species: sulfinamides ($RSONH_2$), mixed disulfides (RSSR′), intramolecular disulfides, and intramolecular sulfinamides (RSONHR′). The nature of the derivatives obtained varied significantly between the three proteins examined here, indicating a strong dependence on the microenvironment of the Cys residues. It is not known if $RSONH_2$ formation is reversible (*16*), but hydrolysis to the corresponding sulfinic acid, RSO_2H (*8*), could result in reduction to the sulfhydryl since sulfinate reductase activity has been reported in vivo (*68*).

In contrast to the protein thiols, HNO oxidizes free Cys to its disulfide, cystine, in near quantitative yield. Thus, bimolecular reaction of the *N*-hydroxysulfenamide intermediate with accessible thiols competes favorably with the unimolecular loss of hydroxide (Scheme 1). Steric hindrance due to the polypeptide likely interferes with intermolecular disulfide formation between Cys residues in proteins, but HNO readily induces protein S-cysteinylation as shown here for HCalB and intrasubunit disulfide formation as seen in GAPDH.

Since S-nitrosation affects protein function, reactions of NO donors with protein-based thiols have received considerable attention recently. BSA (*61*), HCalB (*19*, *45*), and GAPDH (*60*, *61*) are demonstrated targets of NO donors such as GSNO and CysNO. In addition to S-nitrosation, decomposition products invariably found in GSNO samples lead to S-glutathiolation of the proteins studied here (*41*) but not to the formation of protein-based sulfinamides. Also, these proteins exhibit higher reactivity with HNO than GSNO in vitro (*19*, *45*). Thus, the reactions of most protein-based thiols with NO and HNO donors are probably sufficiently different to allow these donors to elicit distinct biological responses (*5*, *20*, *25*). Given the rich chemistry of HNO with protein-based thiols apparent from this survey, further in vitro studies are warranted.

REFERENCES

1. Moncada, S., Palmer, R. M., and Higgs, E. A. (1991) Nitric oxide: physiology, pathophysiology, and pharmacology, *Pharmacol. Rev. 43*, 109−142.
2. Shiva, S., Crawford, J. H., Ramachandran, A., Ceaser, E. K., Hillson, T., Brookes, P. S., Patel, R. P., and Darley-Usmar, V. M. (2004) Mechanisms of the interaction of nitroxyl with mitochondria, *Biochem. J. 379*, 359−366.
3. Shafirovich, V., and Lymar, S. V. (2002) Nitroxyl and its anion in aqueous solutions: spin states, protic equilibria, and reactivities toward oxygen and nitric oxide, *Proc. Natl. Acad. Sci. U.S.A. 99*, 7340−7345.
4. Bartberger, M. D., Fukuto, J. M., and Houk, K. N. (2001) On the acidity and reactivity of HNO in aqueous solution and biological systems, *Proc. Natl. Acad. Sci. U.S.A. 98*, 2194−2198.
5. Miranda, K. M., Paolocci, N., Katori, T., Thomas, D. D., Ford, E., Bartberger, M. D., Espey, M. G., Kass, D. A., Feelisch, M., Fukuto, J. M., and Wink, D. A. (2003) A biochemical rationale for the discrete behavior of nitroxyl and nitric oxide in the cardiovascular system, *Proc. Natl. Acad. Sci. U.S.A. 100*, 9196−9201.
6. Fukuto, J. M., Stuehr, D. J., Feldman, P. L., Bova, M. P., and Wong, P. (1993) Peracid oxidation of an N-hydroxyguanidine compound: a chemical model for the oxidation of N omega-hydroxyl-L-arginine by nitric oxide synthase, *J. Med. Chem. 36*, 2666−2670.
7. Wink, D. A., Feelisch, M., Fukuto, J., Chistodoulou, D., Jourd'heuil, D., Grisham, M. B., Vodovotz, Y., Cook, J. A., Krishna, M., DeGraff, W. G., Kim, S., Gamson, J., and Mitchell, J. B. (1998) The cytotoxicity of nitroxyl: possible implications for the pathophysiological role of NO, *Arch. Biochem. Biophys. 351*, 66−74.
8. Wong, P. S., Hyun, J., Fukuto, J. M., Shirota, F. N., DeMaster, E. G., Shoeman, D. W., and Nagasawa, H. T. (1998) Reaction between S-nitrosothiols and thiols: generation of nitroxyl (HNO) and subsequent chemistry, *Biochemistry 37*, 5362−5371.
9. Spencer, N. Y., Patel, N. K., Keszler, A., and Hogg, N. (2003) Oxidation and nitrosylation of oxyhemoglobin by S-nitrosoglutathione via nitroxyl anion, *Free Radical Biol. Med. 35*, 1515−1526.
10. Sharpe, M. A., and Cooper, C. E. (1998) Reactions of nitric oxide with mitochondrial cytochrome *c*: a novel mechanism for the formation of nitroxyl anion and peroxynitrite, *Biochem. J. 332* (Part 1), 9−19.
11. Saleem, M., and Ohshima, H. (2004) Xanthine oxidase converts nitric oxide to nitroxyl that inactivates the enzyme, *Biochem. Biophys. Res. Commun. 315*, 455−462.
12. Niketic, V., Stojanovic, S., Nikolic, A., Spasic, M., and Michelson, A. M. (1999) Exposure of Mn and FeSODs, but not Cu/ZnSOD, to NO leads to nitrosonium and nitroxyl ions generation which cause enzyme modification and inactivation: an in vitro study, *Free Radical Biol. Med. 27*, 992−996.
13. Poderoso, J. J., Carreras, M. C., Schopfer, F., Lisdero, C. L., Riobo, N. A., Giulivi, C., Boveris, A. D., Boveris, A., and Cadenas, E. (1999) The reaction of nitric oxide with ubiquinol: kinetic properties and biological significance, *Free Radical Biol. Med. 26*, 925−935.
14. Pino, R. Z., and Feelisch, M. (1994) Bioassay discrimination between nitric oxide (NO.) and nitroxyl (NO^-) using L-cysteine, *Biochem. Biophys. Res. Commun. 201*, 54−62.
15. Shoeman, D. W., Shirota, F. N., DeMaster, E. G., and Nagasawa, H. T. (2000) Reaction of nitroxyl, an aldehyde dehydrogenase inhibitor, with *N*-acetyl-L-cysteine, *Alcohol 20*, 55−59.
16. DeMaster, E. G., Redfern, B., and Nagasawa, H. T. (1998) Mechanisms of inhibition of aldehyde dehydrogenase by nitroxyl, the active metabolite of the alcohol deterrent agent cyanamide, *Biochem. Pharmacol 55*, 2007−2015.
17. Kim, W. K., Choi, Y. B., Rayudu, P. V., Das, P., Asaad, W., Arnelle, D. R., Stamler, J. S., and Lipton, S. A. (1999) Attenuation of NMDA receptor activity and neurotoxicity by nitroxyl anion, NO, *Neuron 24*, 461−469.
18. Cook, N. M., Shinyashiki, M., Jackson, M. I., Leal, F. A., and Fukuto, J. M. (2003) Nitroxyl-mediated disruption of thiol proteins: inhibition of the yeast transcription factor Ace1, *Arch. Biochem. Biophys. 410*, 89−95.
19. Tao, L., Murphy, M. E., and English, A. M. (2002) S-nitrosation of Ca(2+)-loaded and Ca(2+)-free recombinant calbindin D(28K) from human brain, *Biochemistry 41*, 6185−6192.
20. Wink, D. A., Miranda, K. M., Katori, T., Mancardi, D., Thomas, D. D., Ridnour, L., Espey, M. G., Feelisch, M., Colton, C. A., Fukuto, J. M., Pagliaro, P., Kass, D. A., and Paolocci, N. (2003) Orthogonal properties of the redox siblings nitroxyl and nitric oxide in the cardiovascular system: a novel redox paradigm, *Am. J Physiol. Heart Circ. Physiol. 285*, H2264−H2276.

21. Fukuto, J. M., Chiang, K., Hszieh, R., Wong, P., and Chaudhuri, G. (1992) The pharmacological activity of nitroxyl: a potent vasodilator with activity similar to nitric oxide and/or endothelium-derived relaxing factor, *J. Pharmacol. Exp. Ther. 263*, 546−551.
22. Pagliaro, P., Mancardi, D., Rastaldo, R., Penna, C., Gattullo, D., Miranda, K. M., Feelisch, M., Wink, D. A., Kass, D. A., and Paolocci, N. (2003) Nitroxyl affords thiol-sensitive myocardial protective effects akin to early preconditioning, *Free Radical Biol. Med. 34*, 33−43.
23. Bai, P., Bakondi, E., Szabo, E., Gergely, P., Szabo, C., and Virag, L. (2001) Partial protection by poly(ADP-ribose) polymerase inhibitors from nitroxyl-induced cytotoxity in thymocytes, *Free Radical Biol. Med. 31*, 1616−1623.
24. Hughes, M. N., and Cammack, R. (1999) Synthesis, chemistry, and applications of nitroxyl ion releasers sodium trioxodinitrate or Angeli's salt and Piloty's acid, *Methods Enzymol. 301*, 279−287.
25. Ma, X. L., Gao, F., Liu, G. L., Lopez, B. L., Christopher, T. A., Fukuto, J. M., Wink, D. A., and Feelisch, M. (1999) Opposite effects of nitric oxide and nitroxyl on postischemic myocardial injury, *Proc. Natl. Acad. Sci. U.S.A. 96*, 14617−14622.
26. Takahira, R., Yonemura, K., Fujise, Y., and Hishida, A. (2001) Dexamethasone attenuates neutrophil infiltration in the rat kidney in ischemia/reperfusion injury: the possible role of nitroxyl, *Free Radical Biol. Med. 31*, 809−815.
27. Miranda, K. M., Dutton, A. S., Ridnour, L. A., Foreman, C. A., Ford, E., Paolocci, N., Katori, T., Tocchetti, C. G., Mancardi, D., Thomas, D. D., Espey, M. G., Houk, K. N., Fukuto, J. M., and Wink, D. A. (2005) Mechanism of aerobic decomposition of Angeli's salt (sodium trioxodinitrate) at physiological pH, *J. Am. Chem. Soc. 127*, 722−731.
28. Feelisch, M., and Stamler J. S. (1996) in *Methods in Nitric Oxide Research* (Feelisch, M., and Stamler J. S., Eds.) pp 71−115, Wiley, New York.
29. Fukuto, J. M., Hobbs, A. J., and Ignarro, L. J. (1993) Conversion of nitroxyl (HNO) to nitric oxide (NO) in biological systems: the role of physiological oxidants and relevance to the biological activity of HNO, *Biochem. Biophys. Res. Commun. 196*, 707−713.
30. Zamora, R., Grzesiok, A., Weber, H., and Feelisch, M. (1995) Oxidative release of nitric oxide accounts for guanylyl cyclase stimulating, vasodilator and anti-platelet activity of Piloty's acid: a comparison with Angeli's salt, *Biochem. J. 312* (Part 2), 333−339.
31. Wilson, E. K. (March 2004) *Chem. Eng. News*, 39−44.
32. Tao, L. (2004) Mechanisms of S-nitrosation and S-glutathiolation and expression and purification of human calbindin D28k, Ph.D. Thesis, pp 42−74, Concordia University, Montreal, Quebec, Canada.
33. Dutton, A. S., Fukuto, J. M., and Houk, K. N. (2004) Mechanisms of HNO and NO production from Angeli's salt: density functional and CBS-QB3 theory predictions, *J. Am. Chem. Soc. 126*, 3795−3800.
34. Zhang, Y., and Wilcox, D. E. (2002) Thermodynamic and spectroscopic study of Cu(II) and Ni(II) binding to bovine serum albumin, *J. Biol. Inorg. Chem. 7*, 327−37.
35. Bulaj, G., Kortemme, T., and Goldenberg, D. P. (1998) Ionization-reactivity relationships for cysteine thiols in polypeptides, *Biochemistry 37*, 8965−8972.
36. Chen, Y. H., He, R. Q., Liu, Y., and Xue, Z. G. (2000) Effect of human neuronal tau on denaturation and reactivation of rabbit muscle D-glyceraldehyde-3-phosphate dehydrogenase, *Biochem. J. 351*, 233−240.
37. Berggard, T., Silow, M., Thulin, E., and Linse, S. (2000) Ca-(2+)- and H(+)-dependent conformational changes of calbindin D(28k), *Biochemistry 39*, 6864−6873.
38. Grossi, L., and Montevecchi, P. C. (2002) S-nitrosocysteine and cystine from reaction of cysteine with nitrous acid. A kinetic investigation, *J. Org. Chem. 67*, 8625−8630.
39. Rubino, F. M., Verduci, C., Giampiccolo, R., Pulvirenti, S., Brambilla, G., and Colombi, A. (2004) Characterization of the disulfides of bio-thiols by electrospray ionization and triple-quadrupole tandem mass spectrometry, *J. Mass Spectrom. 39*, 1408−1416.
40. Di Simplicio, P., Franconi, F., Frosali, S., and Di Giuseppe, D. (2003) Thiolation and nitrosation of cysteines in biological fluids and cells, *Amino Acids 25*, 323−339.
41. Tao, L., and English, A. M. (2004) Protein S-glutathiolation triggered by decomposed S-nitrosoglutathione, *Biochemistry 43*, 4028−4038.
42. Romeo, A. A., Capobianco, J. A., and English, A. M. (2002) Heme nitrosylation of deoxyhemoglobin by s-nitrosoglutathione requires copper, *J. Biol. Chem. 277*, 24135−24141.
43. Parmentier, M., Lawson, D. E., and Vassart, G. (1987) Human 27-kDa calbindin complementary DNA sequence. Evolutionary and functional implications, *Eur. J. Biochem. 170*, 207−215.
44. Romeo, A. A., Filosa, A., Capobianco, J. A., and English, A. M. (2001) Metal chelators inhibit S-nitrosation of Cys beta 93 in oxyhemoglobin, *J. Am. Chem. Soc. 123*, 1782−1783.
45. Tao, L., and English, A. M. (2003) Mechanism of S-nitrosation of recombinant human brain calbindin D28K, *Biochemistry 42*, 3326−3334.
46. Nevona, P. P., Kuncheva, D. S., and Karadakov, B. P. (1978) Spectrophotometric study of copper complexes with diethylene-triaminepentaacetic acid, *Dokl. Bolg. Akad. Nauk 31*, 445−448.
47. van Doornmalen, J., Wolterbeek, H. Th., and de Goeij, J. J. M. (2002) Analysis of copper complex lability using 64Cu-equilibration techniques and free-ion selective radiotracer extraction, *Anal. Chim. Acta 464*, 141−152.
48. Wassarman, P. M., and Major, J. P. (1969) The reactivity of the sulfhydryl groups of lobster muscle glyceraldehyde 3-phosphate dehydrogenase, *Biochemistry 8*, 1076−1082.
49. Hirayama, K., Akashi, S., Furuya, M., and Fukuhara, K. (1990) Rapid confirmation and revision of the primary structure of bovine serum albumin by ESIMS and Frit-FAB LC/MS, *Biochem. Biophys. Res. Commun. 173*, 639−646.
50. Adamczyk, M., Gebler, J. C., and Mattingly, P. G. (1996) Characterization of protein-hapten conjugates. 2. Electrospray mass spectrometry of bovine serum albumin-hapten conjugates, *Bioconjugate Chem. 7*, 475−481.
51. Raftery, M. J., Yang, Z., Valenzuela, S. M., and Geczy, C. L. (2001) Novel intra- and intermolecular sulfinamide bonds in S100A8 produced by hypochlorite oxidation, *J. Biol. Chem. 276*, 33393−33401.
52. Fu, X., Mueller, D. M., and Heinecke, J. W. (2002) Generation of intramolecular and intermolecular sulfenamides, sulfinamides, and sulfonamides by hypochlorous acid: a potential pathway for oxidative cross-linking of low-density lipoprotein by myeloperoxidase, *Biochemistry 41*, 1293−1301.
53. DeMaster, E. G., Redfern, B., Quast, B. J., Dahlseid, T., and Nagasawa, H. T. (1997) Mechanism for the inhibition of aldehyde dehydrogenase by nitric oxide, *Alcohol 14*, 181−189.
54. Stamler, J. S., Simon, D. I., Osborne, J. A., Mullins, M. E., Jaraki, O., Michel, T., Singel, D. J., and Loscalzo, J. (1992) S-nitrosylation of proteins with nitric oxide: synthesis and characterization of biologically active compounds, *Proc. Natl. Acad. Sci. U.S.A. 89*, 444−448.
55. Meier, T. J., Ho, D. Y., and Sapolsky, R. M. (1997) Increased expression of calbindin D28k via herpes simplex virus amplicon vector decreases calcium ion mobilization and enhances neuronal survival after hypoglycemic challenge, *J. Neurochem. 69*, 1039−1047.
56. Thomas, J. A., Poland, B., and Honzatko, R. (1995) Protein sulfhydryls and their role in the antioxidant function of protein S-thiolation, *Arch. Biochem. Biophys. 319*, 1−9.
57. Benitez, L. V., and Allison, W. S. (1974) The inactivation of the acyl phosphatase activity catalyzed by the sulfenic acid form of glyceraldehyde 3-phosphate dehydrogenase by dimedone and olefins, *J. Biol. Chem. 249*, 6234−6243.
58. Padgett, C. M., and Whorton, A. R. (1995) S-nitrosoglutathione reversibly inhibits GAPDH by S-nitrosylation, *Am. J. Physiol. 269*, C739−C749.
59. Allison, W. S. (1976) Formation and reactions of sulfenic acids in proteins, *Acc. Chem. Res. 9*, 293−299.
60. Mohr, S., Stamler, J. S., and Brune, B. (1994) Mechanism of covalent modification of glyceraldehyde-3-phosphate dehydrogenase at its active site thiol by nitric oxide, peroxynitrite and related nitrosating agents, *FEBS Lett. 348*, 223−227.
61. Mohr, S., Hallak, H., de Boitte, A., Lapetina, E. G., and Brune, B. (1999) Nitric oxide-induced S-glutathionylation and inactivation of glyceraldehyde-3-phosphate dehydrogenase, *J. Biol. Chem. 274*, 9427−9430.
62. Grant, C. M., Quinn, K. A., and Dawes, I. W. (1999) Differential protein S-thiolation of glyceraldehyde-3-phosphate dehydrogenase isoenzymes influences sensitivity to oxidative stress, *Mol. Cell. Biol. 19*, 2650−2656.

63. Ishii, T., Sunami, O., Nakajima, H., Nishio, H., Takeuchi, T., and Hata, F. (1999) Critical role of sulfenic acid formation of thiols in the inactivation of glyceraldehyde-3-phosphate dehydrogenase by nitric oxide, *Biochem. Pharmacol. 58*, 133−143.
64. Ravichandran, V., Seres, T., Moriguchi, T., Thomas, J. A., and Johnston, R. B., Jr. (1994) S-thiolation of glyceraldehyde-3-phosphate dehydrogenase induced by the phagocytosis-associated respiratory burst in blood monocytes, *J. Biol. Chem. 269*, 25010−25015.
65. Schuppe-Koistinen, I., Moldeus, P., Bergman, T., and Cotgreave, I. A. (1994) S-thiolation of human endothelial cell glyceraldehyde-3-phosphate dehydrogenase after hydrogen peroxide treatment, *Eur. J. Biochem. 221*, 1033−1037.
66. Simpson, R. B., and Saroff, H. A. (1958) Decrease in sulfhydryl titer of serum albumin, *J. Am. Chem. Soc. 80*, 2129−2131.
67. Claiborne, A., Yeh, J. I., Mallett, T. C., Luba, J., Crane, E. J., III, Charrier, V., and Parsonage, D. (1999) Protein-sulfenic acids: diverse roles for an unlikely player in enzyme catalysis and redox regulation, *Biochemistry 38*, 15407−15416.
68. Jacob, C., Holme, A. L., and Fry, F. H. (2004) The sulfinic acid switch in proteins, *Org. Biomol. Chem. 2*, 1953−1956.
69. Sidman, J. W. (1957) Electronic and vibrational states of the nitrite ion. I. Electronic states, *J. Am. Chem. Soc. 79*, 2669−2675.

BI0507478